Locomotion-related femoral trabecular architectures in Primates

(*Paidopithex rhenanus*, *Pliopithecus vindobonensis*)

Vom Fachbereich Material- und Geowissenschaft
der Technischen Universität Darmstadt

zur Erlangung des akademischen Grades
Doctor rerum naturalium
(Dr. rer. nat.)

genehmigte Dissertation von
Dipl. Geol. Heike Scherf
aus Darmstadt

Referent:	Prof. Dr. F. Schrenk
Koreferent:	Prof. Dr. D. Schumann
Tag der Einreichung:	24.07.2006
Tag der mündlichen Prüfung:	02.02.2007

Darmstadt 2007
D17

Diese Arbeit wurde im Fachbereich Material- und Geowissenschaften, und der Sektion Paläoanthropologie des Forschungsinstitutes Senckenberg unter der Leitung von Prof. Dr. F. Schrenk und Prof. Dr. D. Schumann in der Zeit von Januar 2001 bis Juli 2006 angefertigt.

Acknowledgements

I would like to thank all the people which encouraged and helped me:

Thank you all!

Prof. Friedemann Schrenk and Prof. Dietrich Schumann for enabling and supporting this work.

Dr. Bernd Herkner for his countless advices which helped me to get deeper insight in biomechanics and all related topics, his support in dealing with the various problems which never seemed to decrease, and the assisting discussions.

Dr. Herbert Baaser for making the FEM analyses possible and for his inexhaustible patience with me.

Dr. Felix Beckmann for his kindly assistance in obtaining high resolution CT images with synchrotron radiation.

Dr. Irmgard Pfeifer-Schäller for her patience and support to image the specimens with high resolution CT, despite all trouble.

Prof. Fritz Steininger, Dr. Gudrun Höck, Dr. Christian Meier, Dr. Burkart Engesser, Dr. Gabriele Gruber, who gave me the opportunity to investigate the precious *Pliopithecus vindobonensis* and *Paidopithex rhenanus* fossils.

Dr. Frank Witte and Jens Fischer for their efforts and help to gain deeper insight into bone.

Dr. Jens Franzen and Dr. Gerhard Storch for their valuable remarks on the Eppelsheim site.

Udo Becker and Olaf Vogel for their kind and circumspect help in preparing the specimens.

Anika Hebs, Christine Hemm and Elke Pantak-Wein for their help concerning photographs and the inescapable details which always accompany such a work.

Lilian Ulhaas for her help and critical remarks. She helped me together with Nina Schaller and Meike Schöning always to see a ray of light when it was becoming dark.

And I would like to thank very much Jeremy Tausch for making this thesis readable.

Summary

This work focuses on the influence of locomotor loads on the trabecular architecture of primate proximal femora. A sample of extant primates was used as a comparative base to analyze the trabecular architecture of two Miocene hominoidean species with regard to their habitual hind limb loading. Thereupon, conclusions on the preferred locomotor strategy of the fossil species were drawn. This study is preconditioned by the fact that bones possess the ability of functional, load directed adaptation, and that specific loads are applied on the femur during distinct locomotor modes. These loads are dependent upon body weight and muscle activity (Pauwels 1965, Duda 1996). Different types of locomotion induce different femoral loading, due to the multiple positions of the bodies center of gravity and the various muscles which contract in each phase of locomotion. Therefore, it is hypothesized here that habitual loads which act upon the femur influence the trabecular architecture and therefore the trabecular architecture permits a discrimination of varying locomotor habits.

To obtain accurate 3D data of the proximal femoral trabecular architecture, the specimens were imaged with high resolution computed tomography (CT). Based on these 3D images, the trabecular architecture was structurally described and the features of the trochanter minor region were histomorphometrically analyzed to quantify their characteristics. FEM (Finite Element Method) analyses of models obtained by high resolution (CT) 3D data were conducted and demonstrated the prerequisites for correct simulation of femoral loading conditions in trabecular bone.

The results of the histomorphometric analysis and the structural description of the extant primate sample yielded architectural models of cancellous bone which correspond to their different locomotor behaviors. The same results of the fossil sample were then compared with the extant primate models. This allowed an estimation of the locomotor preferences of the fossil species. Further research on skeletal mechanics and locomotion will improve and refine the analysis of architectural features in cancellous bone. By focusing on internal bony morphology, this study offers a new method which can be used in concert with the classical analysis of locomotor behavior, which relies on external bony morphology. The applied method will also improve the biomechanical analysis of fragmentary fossil material. This work obtained further insight into the functional adaptation of cancellous bone on applied loads and provided information which can be used in pursuing basic research.

Glossary

anisotropy	: different properties in different directions
anterior	: in direction to the front, ventral
E-modulus $[Pa]$ (Young's modulus or stiffness)	: stress to strain ratio resp. the slope of the linear (elastic) part of the stress to strain curve
distal	: limb direction away from the body
isotropy	: same properties in all directions
lateral	: direction away from the midline
medial	: direction towards the midline
microstrain $[\mu E]$	: e.g. 1000 μE cause 1 μm change in length over a total length of 1 mm
ontogeny	: physiological development of an individual
orthotropic	: different properties in the three perpendicular directions
Poisson's ratio	: ratio of transversal to longitudinal strain
poroelasticity	: mechanical theory of fluid/solid interactions in fluid-saturated porous media
properties, apparent	: material properties of a whole bone specimen
properties, tissue	: material properties of a definite type of bone tissue (i.e. trabecular bone)
posterior	: in direction to the rear, dorsal
proximal	: limb direction towards the body
shear modulus $[Pa]$	: ratio of shear stress to shear strain
strain (nondimensional)	: change in length per original length (valid for strain $< 2\%$)
strain energy	: energy absorbed during straining
stress $[Pa]$ (σ)	: force per area ($1\ Pa \mathrel{\hat{=}} N\backslash cm^2$)
toughness $[Pa]$	: amount of energy per volume needed to cause fracture $1\backslash 2$ (yield stress $\times$ yield strain)
transverse isotropy	: same properties in two of the three perpendicular directions
ultimate strength $[Pa]$	: (maximum) stress at which a material fails

yield point	: point on the stress-strain curve which separates the linear part of the curve with elastic deformations from the non-linear part at which plastic deformations occur
yield strain (nondimensional)	: strain value at yield point
yield stress $[Pa]$	: stress value at yield point
yield strength $[Pa]$	: same as yield stress

Contents

Introduction

Bone as a source of information

Bones and teeth are often the only preserved items of extinct animals. Soft tissue remnants, stomach contents or tracks are only preserved under special embedding and fossilization conditions. As paleontology seeks to understand how extinct creatures appeared and existed, fossil bone provides the best source of information to reconstruct their form and locomotor habits. Additional information about their ecology may be gained from the embedding sediment and associated plant fossils. Since the beginning of paleontology, the form and locomotor features of extinct animals were inferred from the external characteristics and proportions of their bones. For locomotor studies, their bone surface morphologies and proportions were compared with those of extant animals. However, fossil specimens are often incomplete or damaged. Locomotion is always performed by associated segments of the body, with each segment influencing the neighboring segment. Therefore, reliable conclusions can only be drawn if almost complete fossil skeletons are used in comparative analyses. In consequence, it is difficult to interpret single fossil bones. In this study, the complex biomechanic interactions between internal bony structures and locomotor loading conditions are investigated. The results provide additional information on the locomotor preferences of extinct animals. It further shows a method of gaining deeper insight into the loading condition of single bones, contributing to a better estimation of their locomotor exercise.

With respect to the extant species, which build the interpretative base of paleontological investigations, it is necessary to understand the relationship between inner bone structures, loading, and locomotion in living animals. For a better understanding of this relationship, comprehensive investigation and interpretation of an organisms biological system is necessary. Today, these investigations are still quite challenging, due to the complexity of biological interactions. Numerous factors contribute to this field of investigation, like morphology, distribution and composition of the articular materials, as well as material properties, metabolic demands, interactions between different materials, and different loading situations. Therefore, a comprehensive and interactive analysis of biomechanics could not be achieved until present time. Such an analysis is additionally hindered by the different investigative emphases, like medical, histological or biomechanical foci, and by the limits of the investigative methods.

In the following some examples of biomechanical-locomotor investigations of primates, with special attention to the skeletal features are listed. One of the first biomechanical investigations of a distinct primate sample group in which skeletal, muscular, and locomotor characteristics were combined was conducted by PRIEMEL (1937). In his work on Plathyrrhini, the skeletal and muscular systems were described, measured, compared between the species, and its locomotion interpreted. He distinguished three types of locomotion for the platyrrhine species, each represented by a species which shows clearly the characteristics of a locomotior type. The leaping type is represented by *Callicebus*, while the slow climbing type is represented by *Alouatta*, and the agile climbing type is represented by *Ateles*. In the work of SCHAFFLER & BURR (1984), the relation between cortical bone characteristics and locomotion was investigated. The osteonal bone fraction of cortical bone and its mechanical loading was therein analyzed. A relationship between osteonal bone fraction and primate locomotion groups was subsequently determined. It was indicated that the locomotor groups of arboreal quadrupedals, terrestrial quadrupedals, suspensors and bipeds can be distinguished by the percentage of osteonal cortical bone. The study of RAFFERTY (1998) was one of the first investigations focusing on the differences in the arrangement of cortical and trabecular bone, and the computed stresses in the femoral neck of various primates. Different distributions of bone in the femoral neck were thereby related to different locomotor behaviors. For example an equal distribution of bone was proposed to be connected to more homogeneous loading conditions. This study was based on accurate 2D x-ray radiographs. However, detailed three-dimensional information about architectural features of cancellous bone could not be obtained at this.

The habitual locomotion of fossils was up to now conventionally interpreted by the outer shape of their bones. Concerning the Miocene hominoideans of this study, locomotor interpretations were made by SIMONS & FLEAGLE (1973), SZALAY & DELSON (1979), BEGUN (1992), and ROSE (1994). The basis for conventional locomotor analysis is the identification of locomotor relevant features. Another, even more important factor is the sufficiency and quality of fossil material. Complications may occur in comparative analyses between fossil and extant specimens if the fossil species practiced a unique locomotor pattern which can not be compared with locomotor patterns in extant forms (DAY 1979). In more recent time MACCHIARELLI et al. (1999), ROOK et al. (1999), and RYAN & KETCHAM (2002) presented a new method for locomotor analysis. It is based upon computed tomography (CT) and focuses on internal bone structures. The first two of the named studies were concerned with the cancellous bone structure of the hip bone of South African australopithecines. The fossil bone structure was compared with the cancellous bone of the hip bone of humans, other extant primates, and the Miocene hominoidean *Oreopithecus bambolii*. The investigations based on 2D CT slices. The therein used CT systems obtained only a resolution of conventional CT systems, making details of the trabecular architecture hardly recognizable. RYAN & KETCHAM (2002) presented a locomotor study about the femoral head trabecular architecture of the two fossil Eocene Omomyinae *Omomys carteri* and *Shoshonius cooperi*. The trabecular architecture was imaged by 3D high resolution CT, histomorphometrically analyzed, and afterwards compared with extant strepsirrhines.

Purpose

The first basic assumption of this work is that loads which act upon the bones of the hind limbs are related primarily to locomotion. The loading conditions of the femur depend on body weight and muscle activity (Pauwels 1965, Duda 1996). The body weight is a constant quantity in the load history. However, the loads applied by the muscles change in accordance to the activity pattern of the muscles. The hip muscles help to balance the body weight on the hind limbs and therefore to stabilize the posture of the trunk. They apply a constant load on hip and femur during various postures. In bipedal postures these muscles alone are responsible for the stabilization. In quadrupedal postures the muscles of the shoulder girdle additionally contribute to the stabilization. During locomotion the center of gravity of the body moves in its relative position to the joints. Therefore, body weight and stabilizing muscles apply correspondingly differing loads on the supporting bones, like the femur. The muscles which contribute to the locomotion itself apply different loads on the femur, too, along with the muscles which stabilize the posture of the trunk. These combined loads represent the main loading conditions of the hind limbs. The actual muscles and the loads they apply differ between the different types and phases of locomotion, as various muscles contract in each phase. The relationship between the mode of locomotion and the resulting general loading conditions is very complex.

The mechanical optimal functionality of bone is still not entirely understood, as outlined by Huiskes (1997). However, the functional adaptation of bone offers a reasonable base for further investigations. It can be assumed that the stresses in the femur which arise during different loading conditions, influence the stress directed modelling and remodelling of the trabecular bone. The second basic assumption of this study is that the mechanically influenced trabecular architecture permits a discrimination of varying locomotor preferences. Rafferty (1998), Scherf (2000) and Scherf et al. (2005) showed that specialized ways of locomotion which cause uniform loading conditions and high loads on the limbs, like leaping e.g., give rise to nonhomogeneous trabecular architectures. This is unlike homogeneous trabecular architectures which evolve under multiple non extreme loading conditions, caused by unspecialized locomotor habits.

The purpose of this work is to analyze and classify the locomotionally related features of the trabecular architecture in the proximal femur of different extant and fossil primate species. These features are further linked to distinct locomotor habits. Based on the results of the

extant species (*Alouatta seniculus*, *Presbytis entellus*, *Papio hamadryas*, *Hylobates syndactylus* and *Homo sapiens*), the trabecular architectures of the two Miocene hominoidea *Paidopithex rhenanus* and *Pliopithecus vindobonensis* were interpreted with regard to their preferred type of locomotion. The effect of the individual life history, like the individual nutrition, the individual time of daily activity e.g., which may be reflected in the trabecular architecture of the extant specimens, was in a first assumption ignored. With regard to the fact that all extant specimens belonged to wildlife animals, an equal mode of locomotion was assumed for each species group.

The present investigation was comprised of several different analyses. The proximal femoral trabecular architecture of the five extant and two fossil were imaged by 3D high resolution computed tomographic (CT). From these images the trabecular architectures were morphologically described and histomorphometrically quantified. Former investigations about locomotor characteristics of primate femora cancellous bone focused on the femoral head and neck (Fajardo & Müller (2001), Ryan & Ketcham (2002a),Ryan & Ketcham (2002b), and MacLatchy & Müller (2002)). In consequence, their locomotor interpretations did not consider the effects of the loads induced directly by the thigh muscles. To take these loads into account the region around the lesser trochanter was chosen as 'Region of Interest' in the histomorphometrical study.

An additional aim of this work was to determine the technical matters for accurate investigations of trabecular architectures by high resolution computed tomography. This technique is now more widely applied in biological and medical sciences to investigate the spatial trabecular network (Goldstein et al. 1991, Goulet et al. 1994, Guldberg & Hollister 1995, Rüegsegger et al. 1996, Guldberg et al. 1997a, Guldberg et al. 1997b, Müller et al. 1998, Stenström et al. 2000, Fajardo & Müller 2001, van der Linden et al. 2001, Ryan & Ketcham 2002a, Ryan & Ketcham 2002b, MacLatchy & Müller 2002). It is a very beneficial tool for these fields of investigation, as it enables analysis of the cancellous bone directly, without destroying samples like in sectioning techniques e.g.. However, at present, no standardized imaging and histomorphometric measurement protocol for high resolution computed tomography exists. This lack of a standard causes inconsistent results and interpretations in similar investigations. A consistent procedure is therefore presented in this study.

The Finite Element Method (FEM) modelling should be used in this work to analyze the mechanical behavior of the trabecular architecture. FEM are commonly applied in biomechanics as shown in chapter 1.2. It was planned to deduce the habitual physiological stress directions and strains which act in the sample femora from their trabecular architectures. This intention is based on the fact that it is still impossible to determine the specific loading environment of any bone of any species (Rubin et al. 1990, Rafferty 1998). Even the specific loading environment in well studied bones like the human femur is inexplicit (Duda 1996).

In the present work, the trabecular architecture of locomotion related bones were investigated in 3D with high resolution computed tomography with an attempt to combine an architectural and mechanical comparative analysis of load and shape in cancellous bone. Due to its interdisciplinary focus, this work contributes to the knowledge regarding the influence of different loads

on skeletal elements and their relation to different modes of locomotion. Similar future investigations of all skeletal elements which are subjected not only to locomotor loads, but all kinds of biomechanical loads will enhance the knowledge about skeletal construction. Together with comparative analyses of the outer bone morphology, this analysis method provides an additional interpretative basis for the locomotor classification of extinct species. Regarding the fact that fossil objects mainly consist of fragmentary skeletal elements, this method can aid in analysis even of single bones with regard to the biomechanical loads which once acted on them.

Chapter 1

Fundamentals

1.1 Constitution and biomechanical role of bone

Studies concerning functional interpretation of skeletal systems should consider the different factors which influence bone structures such as arrangement and morphology of bones, muscles, tendons and ligaments, individual physical condition, habitual loading conditions, nutrition, metabolism as well as the composition of bone and its material properties. Interpretations on this basis are needed, but they are nearly impossible due to the complexity of the different variables. In the following, those factors which are assumed to be mainly related to shape and stabilizing of bone are described.

The fact that bone is a functional structure and that alterations of the loading conditions affect the internal and external bony structures has been common knowledge since the 19^{th} century (Wolff 1892). Since then the biomechanic morphologic and histologic relationships between bone and applied loads has been the subject of more and more detailed analyses (Kummer 1959, Pauwels 1965, Whitehouse & Dyson 1974, Lanyon 1974, Lanyon 1981, Lanyon 1982, Schaffler & Burr 1984, Kleerkoper et al. 1985, Fyhrie & Carter 1986, Carter et al. 1987, Cheal et al. 1987, Frost 1988, Whalen et al. 1988, Frost 1990a, Frost 1990b, Rubin et al. 1990, Turner et al. 1990, Goldstein et al. 1991, Cowin et al. 1992, Chambers et al. 1993, Mullender et al. 1994, Mullender & Huiskes 1995, Salamone et al. 1995, Mullender et al. 1996, Guldberg et al. 1997a, Guldberg et al. 1997b, Huiskes 1997, Stülpner et al. 1997, Schönau 1998, Rafferty 1998, Huiskes et al. 2000, Stenström et al. 2000, Lieberman et al. 2001, Thompson et al. 2001, Tsubota et al. 2002, and many others). These studies initiated basic studies about the mechanical properties of cortical and cancellous bone (Weaver & Chalmers 1966, Lakes et al. 1979, Williams & Lewis 1982, Goldstein 1987, Rice et al. 1988, Odgaard & Linde 1991, Linde et al. 1991, Guldberg & Hollister 1995, Zysset et al. 1999, Keyak & Rossi 2000, Niebur et al. 2000, Wirtz et al. 2000, Morgan & Keaveny 2001, van der Linden et al. 2001, Morgan et al. 2002, van Lenthe & Huiskes 2002, and many others).

The modelling and remodelling process

Both modelling and remodelling processes act to influence the shape of bone. During modelling, bone is built and shaped. The primary shaping mechanism of cancellous bone was described in detail by Aaron & Skerry (1994). They investigated the histological changes which occur during trabecular generation in sheep bone, comparing ontogenetic and healing processes caused by biopsies in adult bone. They found that intratrabecular resorption channels to be mainly responsible for the shaping of the secondary trabecular bone out of the overdense primary network.

During the remodelling process the present bone mass is retained under consistent loading conditions. If the strain level is changed, remodelling adjusts the bone to the new conditions. This happens through the functional loads which act on the bone and influence the remodelling process (Lanyon 1981). For example increased loading will cause bone formation (Chambers et al. 1993). The adjustment of bone structures to varying loads is likely to be the main reason for remodelling. Remodelling is also responsible for the repair of fatigue damages and mineral metabolism (Ott 1996, Huiskes et al. 2000). The remodelling process is based upon directed apposition and resorption of bone (Ott 1996). It is governed by the reciprocal activity of osteoclasts and osteoblasts combined in basic multicellular units (BMUs) or bone remodelling units (BRUs) (Dempster 1992). For adult humans the annual turnover rate of cortical bone is about 2-3 %, whereas approximately 25 % of the trabecular bone is affected (Aiello & Dean 1990 after Eriksen 1986). The first strain based remodelling process simulation on a 3D FEM model of a human proximal femur was presented by Stülpner et al. (1997). In this study simplified loads were subjected to a femur model. Despite the simplified loads physiological correct structures were computed. Some parts of the cortical bone were missing in the finally computed model, probably due to the simplified loading conditions.

A more elaborate theory of modelling and remodelling in healthy mammalian bone is given by Frost (1988, 1990a, 1990b). 'Modelling' sensu Frost (1988, 1990a) is a response to overloading caused by internal and external demands and occurs during growth. When skeletal maturity is reached modelling declines following this theory. The modelling itself happens through the so called 'drift' mechanism. During drift, osteoblast-guided formation adds new bone on defined strain locations while osteoclast-guided resorption removes bone on other strain defined locations. Whether bone is added during the formation drifts or removed during the resorption drifts depends on the type of strain (compression, tension, concave or convex bending), the loading situation of the whole bone, and the local loading situation. Modelling increases when a strain threshold of about 2000 μE (μE: microstrain) (after Frost 1990a) is exceeded for a finite period of time. Below this strain threshold the modelling is retarded. Increased modelling affects longitudinal growth, enlargement of the marrow cavity and the external bone diameter. It also increases the cortical cross-sectional area and influences the shape of bone. Whereas in Frost (1988) the effect of modelling drifts on cancellous bone is expected to be negligible, Frost (1990a) is referring to modelling effects on trabeculae as 'minimodelling'.

The BMU based remodelling is according to FROST's theory (1988, 1990b) a response to underloading. It occurs in juvenile and adult individuals and is responsible for bone turnover and the repair of microdamages. Remodelling is further influenced by physiological constitution, chemical substances, hormones, and nutrition. Depending on the location, remodelling may have different results. On the periosteal surface, bone formation is prevalent than bone resorption, while on the surface of trabeculae and endosteal cortical bone resorption is prevalent than formation. Within haversian canals, resorption and formation are equal. FROST (1988) defines remodelling at a strain threshold of ∼100-300 μE, whereas FROST (1990b) postulates a threshold of 50-100 μE. Below this threshold remodelling is increased, resulting in increased resorption of trabecular and cortical-endosteal bone. This causes an enlargement of the marrow cavity and a thinning of the cortex (FROST 1988). Increased remodelling causes an increase of bone formation on the periosteal surface (FROST 1988 and 1990b). Above the named threshold the remodelling and the described effects decrease. As a consequence of FROST's theory (1988, 1990b), a load directed adaptation of the bone architecture can occur only during modelling. In the adult state, FROST (1988, 1990b) postulates recessive modelling and therefore only very slow adaptation to varying loads. But even if there is no active load directed change in the bone structure during the adult phase, there should be previous adaptation to habitual loads. In the context of this work, only the fact that a load directed adaptation occurs is of importance, not the ontogenetic stage in which it happens.

Nature of loading conditions and other factors which influence bone

The composition of bone is an expression of the loads which are acting upon it. The loads are induced by muscle forces and body weight (PAUWELS 1980, DUDA 1996). The muscle forces cause more significant effects in male humans, whereas body weight is the more prominent factor for female humans (WELTEN et al. 1994). Heredity is an important factor, too, but is estimated to be outbalanced by lifestyle factors (SALAMONE et al. 1995). However, a mathematical model of the relationship between bone density and daily loading history of human calcaneus cancellous bone, proposed by WHALEN et al. (1988), indicates that the stress intensity has a higher influence on bone density and amount of bone than the number of loading cycles. RUBIN et al. (1990) confirmed this statement in their paper which summarized and analyzed former investigations. Another factor which influences the bone mass is the strain rate. The higher the strain rate the greater will be the effect and therefore the increase of bone mass (LANYON 1981). The rise time of loads influences the trabecular bone remodelling, also (GOLDSTEIN et al. 1991). Bone reacts not only to mechanical influences but also to variations of non-mechanical factors, comprising natural agents like hormones, vitamins, ions, amino acids, and artificial agents like hormone and vitamin analogues and drugs. However, it is believed that their influence on skeletal physiology does not exceed that of mechanical factors (FROST et al. 1998).

Allometric effects which influence the loading of bone

The absolute body size of an individual is also of relevancy concerning the locomotor loads. In differently sized animals the forces arising during habitual locomotion "... do not scale in proportion to the body weight." (McNeill Alexander 1985, page 37). As long as it is impossible to determine the actual loading condition of and in a bone, ground reaction forces are the best obtainable measure to describe locomotor loading. The relative ground reaction forces, which refer to body weight, increase with decreasing body size for equal modes of locomotion. Therefore, smaller animals apply higher forces which are several times their body weight on the ground compared to bigger animals. The bigger the animal, the smaller are the relative ground reaction force (McNeill Alexander 1985, Günther 1989). However, Biewener (1989) stated that during strenuous locomotion the muscle and bone stresses of different sized animals stay quite the same. He assumes that this is achieved by size-dependent change in the organization of the limbs. At first sight these two statements may be contradicting, but the consistent stress level in different sized animals can be seen as a consequence of the increasing relative ground reaction forces by decreasing body size and therefore body weight. Lanyon (1981) deduced from experiments with horses and dogs that their actual loading manner stays quite the same throughout different paces and therefore different locomotor styles. Whereas the loading manner stays constant, these experiments showed marked differences in the peak strains of the various locomotor regimes. It is to be noted that these peak strains do not correlate in proportion with pace. The peak strains increase in these animals at the walk - trot transition and decrease when the trot is followed by a canter.

Strain and functional adaptation of bone

It was assumed that the main purpose of the functional adaptation of bone is to reduce strain. A more recent study by Rubin et al. (1990) on cortical bone indicates that the adaptation has the purpose of generating and expanding a definite strain range and type. This is also proposed by Lanyon (1981), who stated that the curvature of some bones accentuates bending rather than decreasing it. Therefore, curvatures seems to be disadvantageous. However, some reasons why it may be beneficial are given by Lanyon (1981). A bone curvature can provide additional space for muscle bodies. There may be further functional need for higher strain levels which are induced by the curvature. The higher strain levels might be needed for the failure free flow of tissue fluid or generation of electrical potentials which may contribute to detection of the actual strain level. Lanyon (1981) stated further that dependent on their position, form, mechanical environment, and physiologic demands (e.g. muscle attachments) different bones may be subjected to different strain ranges. These bone specific features give further rise to different strain types in the various bones. Therefore, it is assumed that the actual bone is in its form and structure adapted to a special strain range and type (Lanyon 1981). The adaptation to a definite strain range might be true for cancellous bone, as well (Keaveny et al. 2001).

The mechanosensoric system in bone

Electrical potentials caused by stress were already discussed in 1964 by Becker et al. as control mechanism of the bone structure. Further possible mechanosensoric systems which enable the functional adaptation of bone are discussed in recent studies (Cowin et al. 1991, Mullender et al. 1994, Mullender & Huiskes 1995, Huiskes 1997, Huiskes et al. 2000, Cowin & Moss 2001). One of these systems is related to electrical potentials which are caused by interstitial fluid flow. However, the most popular hypothesis is that osteocytes act as mechanosensors. Following this hypothesis osteocytes govern remodelling via mechanical stimuli. The stimuli are caused by local strains, which are evoked during loading (Huiskes 1997). A connection between the mechanosensory osteocytes or osteocyte density and the turnover rates in animals of different sizes was proposed by Mullender et al. (1996). It should be noted that strain values measured on whole bone can not be used to estimate the osteocytic strain level at which bone formation occurs. Hollister & Kikuchi (1994) showed in their computational study that principal strains acting on whole bone markedly increases on the osteocytic level.

Adaptation of cortical bone

Cortical and cancellous bone responds in different ways to alterations of the applied loads. Cortical bone, which has the highest load capacity, reacts to differing loading conditions by a variation of its cross-sectional geometry and its density distribution in the cross-section (Pauwels 1965, Lanyon 1974, Adler 1998). This adaptation was computationally simulated by Faust (2001). Schönau (1998) has an different opinion about the adaptation of cortical bone. He postulates that during bone modelling, cortical bone adapts itself to an increase in muscular strength with an increase in cortical thickness and bone geometry but not through alterations of bone density. However, Lanyon (1981) stated that "Local cortical thickness is not proportional to local functional load..." (page 321). Different cortical regions are therefore subjected to different tensile or compressive functional strains and strain magnitudes. He hypothesized that genetic and mechanical factors may interact and give rise to uneven strain distribution.

Adaptation of cancellous bone

Functional adaptation in cancellous bone causes alignment of trabeculae along the principle stress trajectories, which is known as "Wolff's law" (Wolff 1892, Kummer 1959, Pauwels 1965). Proof for the stress related adaptation of cancellous bone was generated by *in vivo* experiments (Lanyon 1974, Goldstein et al. 1991, Guldberg & Hollister 1995, Guldberg et al. 1997a, Guldberg et al. 1997b) and computational studies (Mullender et al. 1994, Mullender & Huiskes 1995, Huiskes et al. 2000, Tsubota et al. 2002). FEM simulations of changes in trabecular architecture of the human proximal femur under single and multiple loading conditions showed a clear relation between architectural changes and apparent principal stresses in different regions of the femur (Tsubota et al. 2002). Goulet et al. (1994) assumed

a relation between the loading environment and the spatial organization of cancellous bone as well as the shape of the individual trabeculae. They further proposed that mechanical loading has a direct influence on the trabecular thickness while the number of trabeculae are affected by hormones or chemical substances.

Mathematical theories about functional adaption

In recent years, numerous studies were carried out on the mathematic formulation of "Wolff's law". The first mathematical formulation of cancellous bone apparent density and alignment was given by Fyhrie & Carter (1986). In their theory they related the adaptation of trabecular orientation and apparent density to variations in the applied stress under static loading conditions. They stated that if this formulation is based on strain energy, the bone is optimizing for stiffness, and if it is based on failure stress, the bone will optimize for strength. The theories of Carter et al. (1987) about the relation of cancellous bone density to strain energy density caused by multiple loading, stress, and fatigue damage based partly on the work of Fyhrie & Carter (1986). Cowin et al. (1992) proposed a dynamic mathematical theory for the adaptation of trabecular bone density and alignment to a stress state which described the temporal change in cancellous bone architecture. Another time-dependent whole bone modelling/remodelling theory was postulated by Beaupré et al. (1990a). Load directed modelling and remodelling were calculated with respect to the available internal and external bone surfaces. This theory was afterwards applied in a simulation of bone density distribution in the human femur. However, the model in this simulation was only a two dimensional model and did not permit changes in the external geometry or consider the actual cancellous bone structure (Beaupré et al. 1990b).

Interrelation between shape and mechanical function of the trabecular architecture

Despite the early formulation of the adaptiveness of cancellous bone to applied loads in the 19^{th} century, investigations of the detailed relationship between loading and the trabecular architecture did not start until the second half of the 20th century, when investigative methods improved. Weaver & Chalmers (1966), in their study about failure strength and mineral content of cancellous bone, were among the first who found that bone strength may be influenced by the spatial organization of the trabeculae along with the mineral content. The scanning electron microscope (SEM) study of Whitehouse et al. (1971) was the first in which the human vertebral trabecular architecture was imaged spatially and combined with 2D surface measurements in high resolution. The subsequent SEM study of Whitehouse & Dyson (1974) emphasized the variability of the trabecular architecture throughout the proximal part of the femur, which is likely to be associated with different loading conditions in the different bone regions. This was extended to the greater trochanter and neck region in human femora by Morgan & Keaveny (2001) and the proximal tibia by Williams & Lewis (1982) using a metallographic microscope. Whitehouse & Dyson (1974) pointed out that quantitative descriptions and interpretations are difficult to interpret with imaging methods that depict the spatial trabecular architecture not as the real 3D structure.

The trabecular architecture and material behavior

Cancellous bone shows anisotropic mechanical properties and behavior. For example its yield strength is higher in compression than in tension while it is lowest under shear conditions (Keaveny et al. 2001). The mechanical properties and behavior of cancellous bone are related to the trabecular architecture as noted by Goldstein (1987), Keaveny & Hayes (1993) and Goulet et al. (1994). Turner et al. (1990) investigated orthotropic E-moduli and shear moduli and found a relationship to the fabric variability of cancellous bone. Fabric variability is proposed to cause anisotropy in the mechanical properties and behavior, like E-modulus, yield strain, yield stress and strength (Keaveny & Hayes 1993, Keaveny 2001, Keaveny et al. 2001, Morgan & Keaveny 2001). The properties depend vice versa on the direction in which they were determined (Goldstein 1987, Goulet et al. 1994).

Calculations of the mechanical behavior of different modelled trabecular networks by Jensen et al. (1990) have shown that within a constant bone volume, the biomechanical competence, i.e. stiffness and strength, of trabecular bone depends on bone density as well as on the architecture of the trabecular bone. This was proposed previously in the studies of Williams & Lewis (1982) and Kleerkoper et al. (1985). This result can be related to Turner's idea (1992) that trabecular architecture changes in order to maintain uniform and isotropic peak strains within the bone. Therefore, it is deducible that a change of the loading conditions, causing a variation in peak strains, changes the requirements for stiffness and strength in trabecular bone. This in turn leads to an alteration in trabecular architecture to retain uniform and isotropic peak strains.

Remodelling itself, which is understood here as turnover processes, influences not only the architecture but also the material behavior of cancellous bone. Differing turnover rates cause different mineralization stages in the bone structure (Mosekilde 1990, van der Linden et al. 2001). These mineralization stages are assumed to give rise to different material properties (van der Linden et al. 2001, Jaasma et al. 2002). Goldstein (1987) estimated that intraspecimen variation of material properties may result from local differing mechanical influences. Following the mechanosensoric system, these influences govern directly the remodelling and therefore the bone turnover. The variations in mineralization should therefore correspond and reflect the mechanical influence.

Functional adaptation and material behavior

Guldberg & Hollister (1995) showed through *in vivo* experiments on immature canid limb bone that mechanical loading influences structural characteristics as well as the material properties of cancellous bone. The E-modulus values of loaded immature bone were quite similar to E-modulus values of mature bone material, while the unloaded immature bone exhibits a markedly lesser E-modulus. Comparable results were obtained in a study about effects of loading during bone repair on canid bone (Guldberg et al. 1997a). Therein, markedly higher values of trabecular plate thickness, cancellous bone connectivity and E-modulus were recorded in loaded bone compared to unloaded bone. Therefore, newly built limb bone in mature canids reaches

the normal physiological mechanical properties during loading, and exhibits a lesser E-modulus when unloaded.

Hydraulic strengthening of bone

Hydraulic strengthening systems in bone could act to stabilize bone and therefore to minimize weight, too. First discussions about such strengthening systems in bone are found in McPherson & Juhasz (1965) and Swanson & Freeman (1966). McPherson & Juhasz (1965) hypothesized a hydraulic strengthening of bone caused by muscle contraction, which effects the blood flow and the marrow pressure. Swanson & Freeman (1966) derived from literature data and their own observations that cortical shaft bone is not hydraulically strengthened. They inferred from either somewhat unphysiological experiments that cancellous bone is not hydraulically stabilized. Draenert (1986) pointed out that bone can be stabilized through the venous system of bone, due to the regulation of venous flow through muscle tone. He further expected that marrow is an important hydraulic strengthening factor. A hydraulic effect caused by the marrow may influence stiffness and strength of bone (Linde et al. 1991). Kasra & Grynpas (1998) modelled the effect of hydraulic stiffening in trabecular bone due to marrow. They found that hydraulic stabilizing increases with loading rate.

Copf & Czarnetzki (1989), Copf & Holz (1994), and Copf (2001) described a membrane system in the proximal end of the femur and at the bone/cartilage boundary of the femoral head. They identified the membranes as part of a hydrodynamic damping system, which regulates the flow of viscous fluid, and consisted of two different membrane-types. The first type occurs only in cancellous bone and consists of collagen lamellae with calcium inclusions which are therefore called CCL-tensulae. At the bone/cartilage boundary the second membrane-type is present, which is probably made of lamellar chondrocyte relics with calcium inclusions (Ccl-tensulae). The CCL-tensulae are rounded with a diameter of 200-400 μm and cover openings between the trabeculae. Due to CCL-tensulae collagenous content they are elastic and therefore can act as buffers in the hydrodynamic damping system. Furthermore they separate red from yellow marrow. The Ccl-tensulae are roundish, too, but with a markedly smaller diameter of 10-20 μm an occur in the lamellar channels of calcified zone. In contrast to the CCL-tensulae, the Ccl-tensulae have openings through which fluid flow might be regulated. They can deform elastically and therefore absorb energy, as well. The literature also mentions another hydraulic damping system in bone, which functions through energy dissipation caused by the frictional resistance of fluid elements during load caused movement (Lakes et al. 1979, Turner & Burr 1993). Although this hypothesis has not been proven (Lakes 2001), the idea of hydraulic stiffening is part of poroelastic bone models (Cowin 2001) and poroelastic remodelling theories (Faust 2001).

Closing remarks

A sample of the broad range of the biomechanics and the constitution of bone tissue, especially of cancellous bone, have been roughly outlined here. The fundamentals and complexity of different topics which contribute to this field are demonstrated. It is evident that in a comprehensive analysis on the biomechanics of bone, all named aspects should be considered. Only under these conditions will extensive functional interpretation of skeletal elements be possible. However, such an comprehensive analysis stays a future challenge as many factors of the single fields of research are not understood and controversial theories about some topics exist.

It is obvious that all aspects described above can not be considered in a single study like the one presented here. Nevertheless, this study makes a contribution to the knowledge about the functional adaptation of cancellous bone.

1.2 FEM (Finite Element Method) and Material Properties of Bone

FEM in Biomechanics

FEM is a numerical method for modelling different material properties and behavior under varying conditions. Therefore, a virtual model of the object to be investigated is generated. This model is composed of small adjoining components. The number of components increase with an increase of the complexity of the model. Changes in external conditions, like loads acting on bone, cause changes on the object and on the single components. These changes are computed as changes to the connections between the components.

Over the last several years FEM has become a common analytical method in biomechanical sciences. It has been used in a variety of investigations. Such as, to model the density distribution in bone (Beaupré et al. 1990b), to investigate stress or strain in bone (Cheal et al. 1987, Goldstein et al. 1991, Guldberg et al. 1997a, Duda et al. 1998), to simulate bone remodelling (Mullender et al. 1994, Mullender & Huiskes 1995, Stülpner et al. 1997, Huiskes 1997, Huiskes et al. 2000, Tsubota et al. 2002), or bone failure (Keyak & Rossi 2000, Niebur et al. 2000), or to examine frictional effects during compression tests (Odgaard & Linde 1991). It is also used to analyze the relationship between mineral distribution and mechanical properties in bone (van der Linden et al. 2001, Jaasma et al. 2002, van Lenthe & Huiskes 2002), or between the trabecular architecture and mechanical properties (Morgan et al. 2002, Newitt et al. 2002), also to examine the effects of bone marrow in hydraulic stiffening of trabecular bone (Kasra & Grynpas 1998), and to estimate strain conduction in bone (Hollister & Kikuchi 1994).

With respect to the complex spatial structure of cancellous bone, Hollister & Kikuchi (1994) and Tsubota et al. (2002) emphasized the need of three dimensional FEM models

to simulate accurately its real spatial structure and properties. Difficulties in generating and computing 3D models of cancellous bone consist mainly in the required PC capacity. The models used at present are based on mathematically computed, geometrically idealized or surface-fitting 3D structures (Kasra & Grynpas 1998, van Lenthe & Huiskes 2002, Tsubota et al. 2002), sectioned images (Niebur et al. 2000, Jaasma et al. 2002, Morgan et al. 2002), or are directly derived from CT or MRT (Magneto Resonance Tomography) images, depicting actual structures (Hollister & Kikuchi 1994, Guldberg & Hollister 1995, Guldberg et al. 1997a, Keyak & Rossi 2000, Borah et al. 2001, van der Linden et al. 2001, Morgan et al. 2002, Newitt et al. 2002). To enable FEM modelling even with powerful workstations the data size of CT and MRT images must be decreased quite often. The decrease of the data size causes a decrease of the original resolution of these images. Nevertheless, it is still impossible to generate a FEM mesh of a whole bone with all internal and external morphologies imaged accurately.

Requirements for FEM modelling - The material properties

In addition to the technical problems, another point of concern with FEM modelling is the objects material properties which can crucially influence the results. The accurate determination of these properties can be very complex. Therefore, care has to be taken in specimen treatment during material testing, in testing method, and local alterations of the bone structure. The following overview covers all the factors which influence the accurate determination of material properties and clarifies the difficulties which arise if a bone structure should be interpreted mechanically correct.

Handling of the testing bone material

The handling of specimens for material testing can cause alterations in bone material properties (Goldstein 1987, Turner & Burr 1993). Under optimal testing conditions, tests are carried out on freshly extracted, untreated bone, in a moist environment at body temperature and with predefined load directions, as advised by Turner & Burr (1993) and Wirtz et al. (2000). Contrary to the assumption of Wirtz et al. (2000), Turner & Burr (1993) mentioned that freezing of fresh bone material after extraction alters the material properties. It seems quite likely that freezing will affect the collagen fibres, as the interstitial fluid will crystallize during this process. Generally it can be assumed that any treatment of bone after removal from the dead body changes the bone material and therefore its properties. For gaining accurate data of the material properties, the bone should ideally be tested immediately after removal under the conditions described above. Additionally, any fluid or viscous substance which under normal physiology is inside the bone has to be prevented from leaking out during testing. With this precaution the conditions of the hydraulic stiffening system as described in chapter 1.1 should be taken into account. The relevancy of considering the hydraulic effects in bone was proofed by Ochoa et al. (1991). Kasra & Grynpas (1998) studied the effect of hydraulic resistance caused by bone marrow in trabecular bone. They noted that vibrational E-modulus analysis may come to different results for bone with and without marrow.

The testing methods

Applied load rate during material testing influences the material properties (Hayes 1986). The method to determine the material properties bear an additional source of error. Rice et al. (1988) described the problems in determining a correct E-modulus value in single trabeculae with computational and experimental methods. These methods obtained data values which differed by as much as 20fold. Odgaard & Linde (1991) noted that different experimental measurement techniques used to determine the E-modulus of cancellous bone provided different values of the E-modulus due to frictional, structural and geometric effects. An optical measurement system used in the former study was used to obtain accurate values. By means of the even more advanced measurement technique of nanoindentation, it is possible to determine local differences in the material properties of bone and can be used in further mechanical analyses. This technique permits the determination of material properties at small, defined localities with a spatial resolution of 1 μm. By using this technique Zysset et al. (1999) showed that E-modulus is influenced by the individual, anatomical location in the bone, and the type of bone tissue (cortical or cancellous bone) which is tested.

Specific features of bone which influences the testing

Zysset et al. (1999) suggested that differences in the material properties between anatomical locations in a bone depend on local differing turnover rates. These in turn cause different grades of mineralization, which are lower in newly formed bone. The grade of mineralization is estimated to influence the material properties vice versa (van der Linden et al. 2001, Jaasma et al. 2002). Mosekilde (1990) showed that new collagen fibers, formed during remodelling are not mineralized. With regard to this finding, testing localities have to be chosen carefully. van der Linden et al. (2001) indicated that by using high resolution computed tomography with synchrotron radiation it is possible to obtain more accurate information about the composition and therefore mineralization grade of trabeculae. As the material properties are influenced by composition and mineralization grade these information might enhance the determination of material properties of trabecular bone. Unfortunately, the available material property data of trabecular bone was determined without taking this information into account.

Zysset et al. (1999) found that differing turnover rates cause further differences in collagen fibre orientations. The orientation is therein assumed to influence the material properties and may therefore contribute to the varying properties of cortical and cancellous bone. The cortical bone had been tested in the longitudinal extension of the osteons and therefore in direction of the collagen fibres. Due to its complex structure, such a testing procedure was not possible for cancellous bone. Goulet et al. (1994) noted that there is a relationship between the testing direction and the determined E-modulus. This source of error can be attenuated when the specimens are tested along the main direction in which the trabeculae are aligned ('on-axis') (Keaveny 2001, Keaveny et al. 2001, Morgan & Keaveny 2001). It is further crucial that material testing procedures of cancellous, as well as of cortical bone, follow special testing protocols to reduce the so called end-artifacts. These occur if the bone specimens have direct

contact with the load plates during testing. The sides of the specimen which are directly loaded become damaged and end-artifacts arise in consequence (KEAVENY et al. 2001, MORGAN & KEAVENY 2001). Further the geometry of the specimen, i.e. the ratio of length to diameter of the specimen, influences the material properties (LINDE et al. 1991, KEAVENY et al. 1993). LINDE et al. (1991) recommended a low ratio between specimen length and diameter for optimal data.

Comparability of material properties of different species

Another difficulty which arises in the context of material properties is pointed out by RICE et al. (1988). It concerns the fact that it is not possible to interpolate material properties from one species to another. KEAVENY et al. (2001) also mentioned critical interspecies differences for E-modulus and ultimate strength. The fact that the amount of bone substance which is present in the testing sample influences the apparent properties surely contributes to the interspecific differences. As RICE et al. (1988) and KEAVENY et al. (2001) focused on human and bovine bone, and therefore on not closely related species, it is estimated that material properties obtained on humans can be used to infer material properties of other primates.

The requirements for an optimal FEM analysis are that only material properties of the investigated species and the anatomical site which is to be examined are used. These material properties should be obtained within testing conditions and methods described above. Some of these requirements could not be fulfilled here, due to the fact that the available values of material properties mostly come from bovine or human bone. Additionally, the actual testing sites of the bones and the testing conditions are often described imprecisely. It is desirable that the above mentioned problems in gaining correct values of material properties for the FEM analysis will be solved in the future with the use of adequate material and methods.

Chapter 2

Material

2.1 Extant Material

The extant sample comprises the five genera *Alouatta seniculus*, *Presbytis entellus*, *Papio hamadryas*, *Hylobates syndactylus* resp. *lar moloch* and *Homo sapiens*. They are represented by two male and two female individuals as far as possible. These genera were chosen by virtue of their preferred mode of locomotion. The main premise was that they exhibit a specialised mode of habitual locomotion, which differs between species. Due to the load directed alignment of cancellous bone, it is assumed that differences in locomotion leave clear signatures in the trabecular architecture. A survey of all examined extant species is given in table 2.1. Right femora are indicated with a "r" behind the collection number and left femora with an "l".

The influence of body weight and allometric effects was also considered in the selection procedure. Therefore, differences in body weight and size were kept as small as possible under the given conditions. Another basic premise was that the body weight of the extant species should be close to the assumed body weight of *Pliopithecus vindobonensis*, estimated at 7 kg (Fleagle 1988). An estimation of the body weight of the second fossil species *Paidopithex rhenanus* is hard to give, as only a single femur is known from this species. However, potential primate species with differing locomotor styles show also different body weights. Therefore, the range of the body weight could not be strictly limited and ranges between 4.5 - 20.9 kg for the non-human primate sample are used.

To exclude influences of unnatural locomotion, or altered nutrition, as they may occur in zoo animals, as well as ontogenetic effects, only femora of adult and wild caught individuals have been used. Due to the fact that no data about the health condition of the wild individuals is available, it was hard to exclude individuals with pathologies. The only possible way was to dismiss those individuals which showed obvious pathological alterations to their skeletons. To ensure uniform conditions it was originally planned to use only femora of the left side of the body. However, in one case (*Hylobates*) a right femora had to been taken instead. In this case

it was additionally necessary to take the femur of a different but similar species from the same genus to obtain a sufficient number of samples.

Table 2.1: Investigated extant species

Species	Collection number	Sex	Origin	Institute
Alouatta seniculus	25 545 l	♀	Amazonas, Rio Manaeapuru, Munduruas	FIS-Z
Alouatta seniculus	25 544 l	♀	Upper Amazonas, Anaty paranei	FIS-Z
Alouatta seniculus	69.19 l	♂	Upper Amazonas	DSA
Presbytis entellus	4734 l	?	India, Molta	UHZ
Presbytis entellus	4743 l	?	India, North Kanara, Gund	UHZ
Presbytis entellus	4745 l	?	India, North Kanara, Mandurli	UHZ
Presbytis entellus	4746 l	?	India, Aushi	UHZ
Papio hamadryas	1.553 l	♀	'Abyssinia'	FIS-Z
Papio hamadryas	Ha VIII 83 l	♂	Ethiopia, Erer Valley near Harar	DSA
Papio hamadryas	Ha VIII 3 l	♂	Ethiopia, Harar	DSA
Papio hamadryas	3212 l	♂	Ethiopia, east of Hadar	PMJ
Hylobates syndactylus	6983 l	♂	Sumatra, Atjeh	DSA
Hylobates syndactylus	52.36. l	♀	Sumatra, Lampongs	DSA
Hylobates lar moloch	47 979 r	♂	?	FIS-Z
Homo sapiens	10 l	♀	-	FIS-PA
Homo sapiens	11 l	♂	-	FIS-PA
Homo sapiens	21 l	♂	-	FIS-PA
Homo sapiens	22 l	♀	-	FIS-PA

The extant sample was provided by the Forschungsinstitut Senckenberg, department of Palaeoanthropology as well as from the Terrestric Zoology department (FIS-PA and FIS-Z) (Frankfurt/Main, Germany), the Dr. Senckenbergische Anatomie (DSA) (Frankfurt/Main, Germany), the Phyletische Museum Jena (PMJ) (Jena, Germany), and of the Institute of Zoology of the University of Hamburg (UHZ) (Hamburg, Germany). The fossil sample includes the Miocene species *Pliopithecus vindobonensis* and *Paidopithex rhenanus* (Table 2.2). The femur of *Paidopithex rhenanus* was put at disposal by the Hessische Landesmuseum Darmstadt (HLMD) (Darmstadt, Germany). The six femora of *Pliopithecus vindobonensis* were provided

by the Naturhistorische Museum Basel (NMB) (Basel, Switzerland) and the Naturhistorische Museum Wien (NMW) (Vienna, Austria).

Table 2.2: Investigated fossil species

Species	Collection number	Origin	Institute
Pliopithecus vindobonensis	O.E. 304 r	Neudorf an der March	NMB
Pliopithecus vindobonensis	O.E. 559 l	Neudorf an der March	NMB
Pliopithecus vindobonensis	O.E. 560 l	Neudorf an der March	NMB
Pliopithecus vindobonensis	1970/1397/22 r	Neudorf an der March	NMW
Pliopithecus vindobonensis	1970/1397/23 l	Neudorf an der March	NMW
Pliopithecus vindobonensis	1970/1398/2 l	Neudorf an der March	NMW
Paidopithex rhenanus	Din 45 r	Eppelsheim	HLMD

The following systematic classification of the different sample species is according to Szalay & Delson (1979). This reference contains former and alternatively used designations, too.

2.1.1 *Alouatta seniculus* - Red howler monkey

Order: **Primates**, Linnaeus 1758
Suborder: Haplorrhini, Pocock 1918
Infraorder: Platyrrhini, Geoffroy Saint-Hilare 1812
Family: Atelidae, Gray 1825
Subfamily: Atelinae, Gray 1825
Genus: *Alouatta*, Lacépède 1799
Species: *Alouatta seniculus*, Linnaeus 1766

Table 2.3: Profile *Alouatta seniculus* (Ashton & Oxnard 1964, Langdon 1986, Welker & Schäfer-Witt 1988)

Habitat	HTL*	Weight	Food	Locomotor classification
in the north of South America	♂: 49-72 cm ♀: 46-57 cm	♂: 6.5-8.1 kg ♀: 4.5-6.4 kg	leaves, partly ripe fruits and flowers	semibrachiators

HTL*: Head to trunk length

Originally it was planned to use femora of *Alouatta villosa*, the guatemalan howler monkey, in this study. Its body weight of $\sim$ 9 kg for females and $\sim$ 10.9 kg for males (Welker &

Schäfer-Witt 1988) is closer to the range of body weights of the other examined species. Due to the difficulties finding femora of adult, healthy, and wild caught individuals of this species, the red howler monkey *Alouatta seniculus* (Figure 2.1, Table 2.3) was taken instead.

Howler monkeys are named after their habit of common howling to mark present whereabouts and also in situations of danger. Most time is spend in the treetops and they are rarely seen on the ground. They spend up to 80% of their active daytime resting and travel only short distances (Welker & Schäfer-Witt 1988). Field studies on howler monkeys were started by Clarence Ray Capenter in the early 1930ies. Observations on the different species of howler monkey have yielded similar results (Carpenter 1934, Welker & Schäfer-Witt 1988, Bergeson 1998). Therefore, it was considered to be acceptable to refer to these observations for the locomotor and positional description of *Alouatta seniculus*.

Figure 2.1: Red howler monkey (*Alouatta seniculus*), © Roger Neckles 2004

Locomotor behavior

Compared to other primates, howler monkeys climb and walk slowly and carefully, using their prehensile tail like an extra grasping limb to secure themselves during movement. The body is predominately held in a pronograde position. The substrate is grasped with the forepaws between the second digit (index finger) and third digit, while these two digits are spread up to nearly 180°. The feet seize a branch between the toe and the other digits. Leaping is rarely observed and they prefer to climb from one tree to an other. If required they can perform jumps over 3 - 4 m. To accomplish a jump they push off the body with their hind limbs, while one or both hands initially leave the substrate. During the jump the hands reach out to seize a branch at the final destination. Finally the feet and the prehensile tail loose the grip on the branch. The main push off force seems to come from the hind limbs with only a little help by the fore

limbs. Even though howler monkeys move slowly most of the time, they can retire quickly in situations of danger (Krieg 1928, Carpenter 1934, Welker & Schäfer-Witt 1988, own observations from the wild life film Die Affen - Neuweltaffen in Südamerika 1990).

During quadrupedal stance and gait the fore and hind limbs are placed under the body axis, while knees and elbows are flexed to bring the center of gravity closer to the substrate and by this into a more stable position. During walking and climbing no more than two limbs are lifted from the substrate at the same time. The movement begins with the fore limbs. While shoulder muscles pull the body foreword the hind limbs push the body by tension of the extensors (Grand 1968a). A detailed description of the single movements of the hind limb elements during quadrupedal gait is given by Grand (1968b). The howler monkeys show a broad range of sitting, lying, and resting postures with no preference to a definite posture. During feeding and playing they may suspend themselves partly or completely by their tails, while suspension on a single limb was not observed (Krieg 1928, Carpenter 1934, Grand 1968a and 1968b, Bergeson 1998).

2.1.2 *Presbytis entellus* - Hanuman langur

Order: **Primates**, Linnaeus 1758
Suborder: Haplorhini, Pocock 1918
Infraorder: Catarrhini, Geoffroy Saint-Hilare 1812
Family: Cercopithecidae, Gray 1821
Subfamily: Colobinae, Blyth 1875
Genus: *Presbytis*, Eschscholtz 1821
Species: *Presbytis entellus*, Dufresne 1797

Table 2.4: Profile *Presbytis entellus* (Langdon 1986, Vogel & Winkler 1988)

Habitat	HTL	Weight	Food	Locomotor classification
India, Nepal, Sri Lanka	51-108 cm	♂: 9-20.9 kg ♀: 7.5-18 kg	vegetarian, occasionally insects	runners and leapers

The Hanuman langurs (*Presbytis entellus*, Figure 2.2, Table 2.4) inhabit a large area, reaching from the high mountains of Nepal over the semi-deserts of north-west India to the rain forests of Sri Lanka. In this way they cover nearly all ecological regions. In many areas they often inhabit cities or temple complexes. Depending on their environment they live predominately arboreal or terrestrial (Vogel & Winkler 1988). It seems reasonable to expect differences in the trabecular architecture between predominately arboreal and predominately terrestrial living individuals. At least two of the herein used specimens (UHZ 4745 l, UHZ 4743 l) lived certainly

in the cost region of Karnataka in south-west India. This region is covered by subtropical forest, indicating that these individuals lived predominately arboreal. A detailed description of the locomotor and positional behavior of predominately arboreal *Presbytis entellus* is given in the comprehensive work of Nikolei (2002). The therein described group lived in the southern part of Nepal in a subtropical forest region at an altitude of 300 m.

Figure 2.2: Group of Hanuman langurs (*Presbytis entellus*) (Vogel & Winkler 1988)

Locomotor behavior

On average Hanuman langurs are 3.5% of their active day hours locomotor active, while they spend over 90% with sitting. Lying and standing occur more rarely. They are frequently on the ground and their locomotor activities take place in equal shares in the trees and on the ground. The terrestrial and arboreal locomotion involves quadruped walking, trotting, and galloping. Walking is the most frequent locomotor mode, especially in trees. Walking and trotting is accomplished by a symmetric lateral limb movement. Asymmetric limb coordination can be observed during galloping, including real flight phases. A further preferred arboreal locomotion mode is leaping. It is occasionally performed on the ground, as well. The propulsive power for the leaps is mainly provided by the hind limbs. Leaps up to 10 m between trees were observed (Figure 2.3). The flexibility of the substrate is often used as a spring board to enhance performance. During touch down, the fore and hind limbs are used. To reduce shock on the joints during touch down, the impulse force of the leap is transformed into motion force for quadrupedal walking, as far as the environment permits such a transformation. Along with leaping, another load intensive locomotor activity of *Presbytis entellus* consists of dropping down from a branch after hanging from one or both forearms (Nikolei 2002).

A further common kind of locomotion is climbing. Vertical substrate climbing is performed by pushing the body upwards with the hind limbs while the fore limbs grasp the substrate.

Thinner branches are climbed in a walking mode with diagonal limb coordination. Downward climbing is accomplished with hind legs coming down first. Hanuman langurs also perform bipedal walking occasionally. This mode involves the legs being spread wide apart with the arms sometimes used to balance the body (Nikolei 2002).

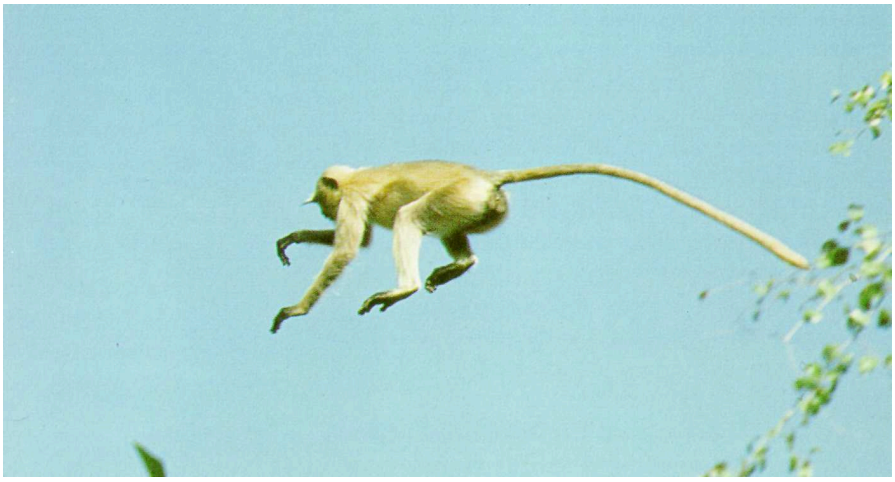

Figure 2.3: Leaping Hanuman langur (*Presbytis entellus*)(Vogel & Winkler 1988)

2.1.3 *Papio hamadryas* - Sacred baboon

Order: **Primates**, Linnaeus 1758
Suborder: Haplorhini, Pocock 1918
Infraorder: Catarrhini, Geoffroy Saint-Hilare 1812
Family: Cercopithecidae, Gray 1821
Subfamily: Cercopithecinae, Gray 1821
Genus: *Papio*, Müller 1773
Species: *Papio hamadryas*, Linnaeus 1758

Table 2.5: Profile *Papio hamadryas* (Langdon 1986, van Hooff 1988)

Habitat	HTL	Weight	Food	Locomotor classification
southwest Arabia, west Africa	♂: 60-94 cm ♀: 50-65 cm	♂: ∼ 18 kg ♀: ∼ 10 kg	grass, roots, seeds, nuts, fruits, invertebrates and small vertebrates	runners and walkers

The sacred baboons (*Papio hamadryas*, Table 2.5) live, like all baboons, predominately terrestrial. Only at nightfall do they climb cliffs or trees. In southwest Arabia and Ethiopia, where all examined specimens are from, sacred baboons inhabit dry semiarid regions and rocky barren landscapes up to 2000 m (van Hooff 1988). The average body weight for male individuals of $\sim$ 18 kg was exceeded by two specimens (Ha VIII.83 l ♂ with 24 kg and Ha VIII 3 l ♂ with 19.6 kg). Along with differences in body size and weight male sacred baboons show further sexual dimorphism by the lighter colour and pronounced mane on the head and upper part of the body (Figure 2.4) (van Hooff 1988).

Figure 2.4: Male and female sacred baboons (*Papio hamadryas*)(Barrett 2000)

Despite the fact that the social behavior of *Papio hamadryas* is well studied, no detailed description about the positional and locomotor habits of this species seems to be available. The following descriptions are based on the observations of Hall (1962) on Chacma baboons (*Papio ursinus*) from southern Africa and my own observations made from two wild life films on yellow baboons (*Papio cynocephalus*) (Menschen und Tiere - Bei den Pavianen, Die Affen - Paviane und Mantelaffen in Afrika 1990). As all baboons are quite similar in their locomotor performances and yellow and sacred baboons in particular inhabit comparable habitats, this substitution is estimated to be suitable.

Locomotor behavior

Most of the time baboons walk quadrupedally terrestrially and arboreally. When walking on branches neither hands nor feet seem to clutch the substrate. During walking the limbs are

coordinated diagonally. The more powerful locomotor modes of pseudo-galloping and trotting are only performed on the ground (Figure 2.5). They are accomplished by an asymmetric limb coordination, while the forelimbs make first contact with the ground before hind limbs touch down. The delay between the left and the right site of the fore and hind limbs hitting the ground decreases with increasing speed.

Figure 2.5: Cantering yellow baboons (*Papio cynocephalus*) (VAN HOOFF 1988)

Juveniles seem to climb or leap more often than adults. They also semibrachiate across short distances. During climbing, only the hands clutch the substrate while the feet are placed flat. This manner contrasts with the climbing fashion of the howler monkeys which clutch the substrate with hands and feet. Yellow baboons are observed to climb vertically with the hind limbs pushing the body upwards by successional leaps, while the hands seize the log like the Hanuman langurs. Shorter distances on vertical substrates are climbed in a kind of pace. A similar upward leaping fashion was observed by HALL (1962) as Chacma baboons climbed rockfaces. However, on almost vertical slopes he described a human-like climbing fashion. When descending steep cliffs or rocks baboons might climb sideward and secure themselves with their hands which are kept above the level of their feet. A faster way of ascending is accomplished by a 180° rotation of the body. First the upper part of the body goes down and sizes a secure grip with the hands and then the rest of the body swings downward. The rare leaps are rather short and performed carefully. The forearms are put forward while leaping to seize a first hold on the other side. The same habit was observed when Chacma baboons have fallen down accidentally in a way that Hall described as a "... cat-like four-point..." (page 217) landing. In yellow baboons it was sometimes observed that they let themselves drop from a higher towards a lower branch. During the fall they put the arms downward to grip the lower substrate. The common terrestrial and arboreal resting posture of baboons is to lie down or to sit upright while the hind limbs are adducted. On the ground they sometimes also stand bipedal. The legs are thereby more or less extended (Figure 2.6).

Figure 2.6: Bipedal standing male sacred baboon (*Papio hamadryas*) (VAN HOOFF 1988)

2.1.4 *Hylobates syndactylus / lar moloch* - Siamang / Silvery gibbon

Order: **Primates**, LINNAEUS 1758
Suborder: Haplorhini, POCOCK 1918
Infraorder: Catarrhini, GEOFFROY SAINT-HILARE 1812
Family: Hominidae, GRAY 1825
Genus : *Hylobates*, ILLIGER 1811
Species: *Hylobates syndactylus*, RAFFLES 1821
Species: *Hylobates lar*, LINNAEUS 1771

Table 2.6: Profile *Hylobates syndactylus* (PREUSCHOFT 1988)

Habitat	HTL	Weight	Food	Locomotor classification
Sumatra, southern part of Malakka	♂: 46.8-59.5 cm ♀: 43.8-63.0 cm	∼ 11 kg	leaves (up to 48%), fruits, insects, eggs, small vertebrates	brachiators

The forests of southeast Asia are the home of the Gibbons. Two of the specimens included in this project belong to the genus *Hylobates syndactylus*, commonly called Siamang or great

Table 2.7: Profile *Hylobates lar moloch* (Preuschoft 1988)

Habitat	HTL	Weight	Food	Locomotor classification
western part of Java	44-64 cm	5-6 kg	mainly fruits, also leaves	brachiators

gibbon (Table 2.6). A third specimen of wild caught adult gibbon could only be obtained from a silvery gibbon (subspecies *Hylobates lar moloch*, Audebert 1798 after Groves 1972, Table 2.7)). The silvery gibbon has a body size similar to the Siamang but with body weight of 5-6 kg and so below the average weight of a Siamang ($\sim$ 11 kg) (Preuschoft 1988). Only a right femur was accessible from this specimen. However, as the locomotor modes of all gibbons are quite similar, the results should not be markedly affected by this.

Gibbons live arboreally and brachiate as their predominant mode of locomotion (Figure 2.7). Brachiating gibbons might "fly" distances up to 10 m (Preuschoft 1988). A detailed description of the brachiation of gibbons is given in the wild life observations of Carpenter (1940). Therein he noted that the gibbon tucks up the legs during brachiation. He also found out that many gibbons have healed fractures, which he suspected are caused by accidental falls. Fleagle (1976) states that the "Siamang usually brachiate along supports rather than between them." (page 247). He observed that the fast, ricochetal kind of brachiation is more frequently practised by smaller gibbon species and juvenile Siamang than by adult Siamang.

Figure 2.7: Brachiating lar gibbon (*Hylobates lar*) (Preuschoft 1988)

Locomotor behavior

Climbing along with brachiating is the most common mode of locomotion for gibbons. The forelimbs seem to dominate this locomotor mode. However, climbing is more often observed in Siamangs than in smaller gibbons. Even though climbing requires the use of three or all four limbs, a common quadrupedal gait is rarely observed, for example only on long and even branches (Fleagle 1976, 1980). The hind limbs are loaded during bipedal walking, also. During this locomotor mode the hind limbs are flexed at the knee and the hip joints. The arms may be stretched out sideways over the level of the head like a balancing pole, or are put to the ground in a kuncklewalking fashion while the body is put in an orthograde position. Unlike human walking, bipedal locomotion of gibbons also contains bouncing elements and fast movements. Details of the bipedal walk of gibbons were investigated by Prost (1967), Okada (1983), and Okada (1985) for example. A comprehensive study on this issue has been done by Vereecke (2006). Gibbons use bipedal locomotion from 5 to 12% of their active time and therewith more often compared to all other non-human primates. Bipedal walking is preformed in trees and during the rare time which they spend on the ground (Carpenter 1940, Fleagle 1976, Napier 1976, Preuschoft 1988, Vereecke 2006).

Downward leaps belong to the locomotor repertoire of gibbons, too. Carpenter (1940) observed leaps at the end of a normal swinging phase and like Fleagle (1976) he also noted leaps out of a resting position. The arms seem to provide the main take-off force by pulling the body forward. In this way gibbons may leap over a horizontal distance of up to 10 m, while they can cover more than 20 m in vertical distance. Fleagle (1976) describes further deliberate downward drops between different branch levels. Sitting, hanging, reclining, lying and upright standing are among the frequent postures of gibbons (Carpenter 1940, Fleagle 1976, Fleagle 1980). Baldwin & Teleki (1976) give more detailed descriptions of the various modes of gibbon locomotor and positional behavior which were just outlined here.

2.1.5 *Homo sapiens* - Humans

Order: **Primates**, Linnaeus 1758
Suborder: Haplorhini, Pocock 1918
Infraorder: Catarrhini, Geoffroy Saint-Hilare 1812
Family: Hominidae, Gray 1825
Genus: *Homo*, Linnaeus 1758
Species: *Homo sapiens*, Linnaeus 1758

Due to its highly specialized mode of bipedal locomotion, *Homo sapiens* was included in the extant sample. The specimens were provided to the department of Paleoanthropology of the Forschungsinstitut Senckenberg by the Rechtsmedizinische Institut of the University of Frankfurt, Main (Germany). In contrast to the non-human primate specimens, specific declaration about weight, size, and age were available. The size was unfortunately measured as full body

height and not as HTL, like in the data of the non-human primates. The data are listed in table 2.8.

Table 2.8: Specimen data

Collection number	Sex	Body weight	Body height	Age
FIS-PA 10 l	♀	64 kg	166 cm	50 years
FIS-PA 11 l	♂	95 kg	191 cm	69 years
FIS-PA 21 l	♂	106 kg	189 cm	54 years
FIS-PA 22 l	♀	58 kg	158 cm	22 years

The human locomotor system is a focus in some medical sciences. Many studies exist about muscle activities, motion of body segments, calculated or measured joint forces, and internal bone loads and strains (for example Crowninshield et al. 1978, Soderberg & Dostal 1978, Hodge et al. 1989, Kotzar et al. 1991, Bergmann et al. 1993, Duda 1996, Duda et al. 1998, Heller et al. 2001a, Heller et al. 2001b). They build the scientific base for biomechanic studies like the ones lined in chapter 1.1 and 1.2.

The morphological conditions for primate bipedalism of the hip and the lower extremities have been the focus of comparative studies for decades (for example Zuckermann et al. 1973, Lovejoy 1984, Preuschoft & Witte 1993, Marchal 2000). Human bipedalism has also been compared to biped habits of non-human primates (Prost 1967, 1980, Ishida et al. 1985, Kimura 1985, Okada 1985, Yamazaki 1985). Social reasons for bipedalism were recently investigated (Jablonski & Chaplin 1993). One of the first discussions about bipedalism in non-human primates actually began at the end of the 19^{th} century and regarded the extinct *Paidopithex rhenanus* (see Chapter 2.2.2).

Locomotor behavior

Bipedalism is just one example of the different and extreme modes of habitual locomotion investigated here. Only the basics about human locomotion, comparable to the information provided about the other species, are given. It must be noted that humans mostly walk and are therefore assigned as bipedal walkers. Running and climbing are performed to a lesser extent in daily life. The preferred postures are standing, sitting and lying. More variations in human locomotion and posture surely exist but the above named habits are the most common and in the context of this work therefore the only relevant ones.

2.2 Fossil Material

2.2.1 *Pliopithecus vindobonensis*

Order: **Primates**, Linnaeus 1758
Suborder: Haplorhini, Pocock 1918
Infraorder: Catarrhini, Geoffroy Saint-Hilare 1812
Family: Pliopithecidae, Zapfe 1960
Genus: *Pliopithecus*, Gervais 1849
Species: *Pliopithecus vindobonensis*, Zapfe & Hürzeler 1957

The species *Pliopithecus vindobonensis* belongs to the family Pliopithecidae, which are known from various Miocene localities from western Europe to southern China. The genus *Pliopithecus* was predominately located in Europe during the middle and late Miocene and represents the oldest group of fossil catarrhines in Europe. One species known from middle Miocene deposits of northern China is also attributed to *Pliopithecus*. Due to numerous findings from a fissure near Neudorf an der March (Děvínská Nová Ves, Slovakia), *Pliopithecus vindobonensis* is the best known of all *Pliopithecus* species (Szalay & Delson 1979, Fleagle 1988, Andrews et al. 1996) (Figures 2.8, 2.9). It is estimated that *Pliopithecus vindobonensis* had a body weight of 7 kg (Fleagle 1988).

The investigated specimens belong to the above mentioned upper Miocene findings of Neudorf an der March, which yielded not only the type specimen but also numerous other fossil remnants of *Pliopithecus vindobonensis*. They were accurately described and analyzed in the comprehensive work of Zapfe (1960). Therein a mean trunk length of 38 cm was computed for individual I and II, under the assumption that both were male individuals. The investigated sample consists of the right femur of individual I (O.E. 304, Zapfe 1960 C23) and two proximal fragments of left femora (O.E. 560, Zapfe 1960 S. 168 ff., O.E. 559, Zapfe 1960 C34), provided by the Naturhistorische Museum Basel. The right (1970/1397/22) and left (1970/1397/23) femur of individual II (Zapfe 1960 C39) and another fragment of a proximal left femur (1970/1398/2, Zapfe Fig. 79) are included in this study by permission of the Naturhistorische Museum Wien. The taxonomic classification of *Pliopithecus* is still not clear. Zapfe (1960) argued on the basis of proportional relations and morphology of the skeletal elements that *Pliopithecus* belongs to the original group which gave rise to the extant Hylobatinae. Simons & Fleagle (1973) rejected this view and interpreted these features as signs of an early hominoid stage, separate from modern forms. Morphometric analysis on the proximal part of the femur by McHenry & Corruccini (1976) pointed out the similarities of *Pliopithecus vindobonensis*, *Paidopithex rhenanus*, and *Hylobates*. The authors estimated that both fossil species belong to the Hylobatinae. A multivariate analysis of the shoulder joint of *Pliopithecus vindobonensis*, done by Ciochon & Corruccini (1977) contradicted this interpretation and showed that the shoulder joint of *Pliopithecus* is most similar to *Presbytis rubicunda* and *Cebus apella*. Therefore, they rejected the classification of *Pliopithecus* as a hominoid and defined it as a catarrhini *incertae*

Figure 2.8: Skeletal reconstruction of *Pliopithecus vindobonensis* (Zapfe 1960)

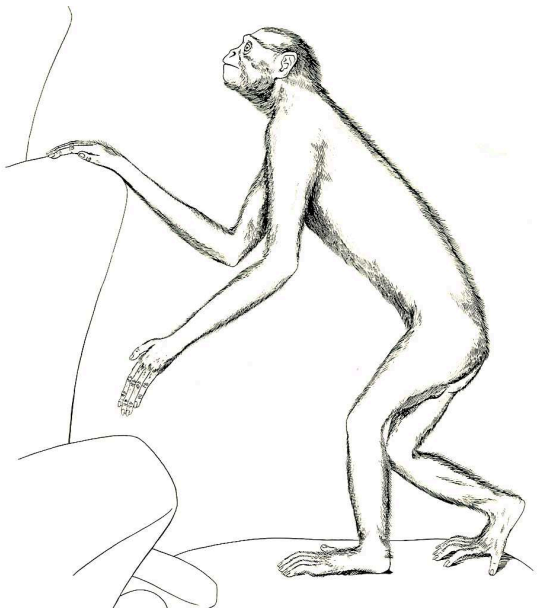

Figure 2.9: Reconstruction of the living appearance of *Pliopithecus vindobonensis* (Zapfe 1960)

sedis. However, Szalay & Delson (1979), Fleagle (1983), Fleagle (1988), and Conroy (1997) assigned *Pliopithecus* again to the hominoids, while Martin (1990), and Andrews et al. (1996) defined it as a catarrhine.

Locomotor interpretation

Considering the locomotion of *Pliopithecus vindobonensis* Zapfe (1960) noted that the femur shows characteristics comparable with platyrrhine and hylobatine femora. He concluded on basis of skeletal element morphology that *Pliopithecus vindobonensis* was a locomotor generalist (Figures 2.8, 2.9). Following his interpretation, this Miocene species did not live strictly arboreally and might have moved frequently quadrupedal on the ground. He argued that the site at which the fossil was found, along with the reconstructed palaeoecology of a dry forest, would support this interpretation. He argued that *Pliopithecus vindobonensis* could have deliberately gone in the fissure where its remnants were found while searching for water and was trapped inside.

However, on the basis of the last sacral vertebra Zapfe estimated that *Pliopithecus vindobonensis* might have had three or four caudal vertebrae. Ankel (1965) argued from the dimensions of the sacral canal that this species had a tail consisting of approximately ten to fifteen caudal vertebrae. The existence of a tail might have implications for locomotor considerations, as it supports some of the following locomotor interpretations. Simons & Fleagle (1973) argued that the shape of the *Pliopithecus vindobonensis* femur shows characteristics which are common in primates with suspensory locomotion. They stated further that features which are indicating quadrupedal running or leaping are not present. With respect to its postcranial anatomy, they considered that *Pliopithecus vindobonensis* practiced a locomotor style comparable to howler monkeys (*Alouatta*), spider monkeys (*Ateles*), and wooly monkeys (*Lagothrix*), which are all semibrachiators with a prehensile tail. The two latter ones are quite agile species compared with the howler monkeys (Ashton & Oxnard 1964). Szalay & Delson (1979) confirmed this interpretation partially, comparing the skeletal structure of this fossil with the atelines. Following their argumentation *Pliopithecus vindobonensis* was "..an agile arborealist, engaging in some suspensory postures as well as running, climbing and leaping." (page 454). But they doubt that it had a tail like Ankel (1965) presumed. They also disagreed with Zapfe's interpretation of the site as an index for terrestrial locomotion. After their opinion the *Pliopithecus vindobonensis* individuals were washed into the fissure.

Yet, on the basis of overall anatomy, with special attention to the morphological features of the hind limbs, Fleagle (1983) estimated that *Pliopithecus vindobonensis* was a suspensory, tailless arborealist, comparable to *Ateles* (Figure 2.10). He emphasized that there are no indications for more load intensive locomotor behaviors like extensive ground or arboreal quadrupedalism or leaping habits. Langdon (1986) affirmed this assumption by his analysis of the anatomy of primate foot bones. However, he noted that the foot bones of *Pliopithecus* show features which are typical for climbing behavior. The interpretation of Rose (1994) did not limit the locomotor repertoire as strictly as the latter two authors. Rose assumed on the

basis of limb proportions and bone morphology that *Pliopithecus vindobonensis* practiced other forms of quadrupedal locomotion along with climbing and suspensory behavior.

The above interpretations of the locomotor behavior of *Pliopithecus vindobonensis* outline the differing opinions surrounding its locomotor behavior. Even though the latter investigations agree that this species lived arboreally and dispute the importance of suspensory locomotion, a final answer to the preferred locomotion of *Pliopithecus vindobonensis* is still not achieved.

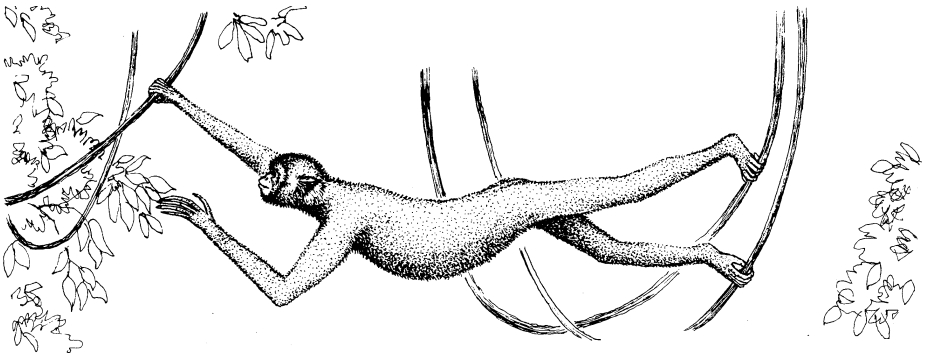

Figure 2.10: Reconstruction of the locomotor habits of *Pliopithecus vindobonensis* (Fleagle 1988)

Description of the site of Neudorf an der March

The fissure of Neudorf an der March is located east of the nearby Vienna Basin and runs approximately parallel to the eastward boundary of the basin. This fact supports the assumed contemporary evolution of these two structures. The fissure is filled with boulders of the adjoining limestone bedrock and fine sediments. These sediments acting as cement for the boulders and consist predominately of russet colored clay. There are no indications that the boulders were transported over some distance or for fluviatile rearrangement of the fossils. The site is therefore interpreted as parautochthonous. The fossils were found in clay deposits and were partly crusted with sinter. The sinter crusts indicate that the fossils were not immediately embedded in the clay. Yet, the fissure seems to have been filled quickly, as the infillings do not show a stratigraphic order. It is assumed that the individuals were trapped in the fissure alive and that the site shows a thanatocoenosis. This is supported by the fact that bite marks could not be found on the fossil bones. Near the main fissure several similar fissures outcrop and have yielded further fossil material of *Pliopithecus vindobonensis* (Zapfe 1960).

The fossil material of the Neudorf fissure is dated in the transition of the Mammal Neogene Zone MN 5 to MN 6, whereby the exact position is still under debate (Daxner-Höck 1998). This time comprises the transitional period from the European Land Mammal Mega Zone of the Orleanian to the Astaracian (Steininger 1999). The *Pliopithecus vindobonensis* fossils from Neudorf an der March could therefore be aged to approximately 15 Ma.

2.2.2 *Paidopithex rhenanus*

Order: **Primates**, Linnaeus 1758
Suborder: Haplorhini, Pocock 1918
Infraorder: Catarrhini, Geoffroy Saint-Hilare 1812
Family: Hominidae, Gray 1825
Genus: *Dryopithecus*, Lartet 1856
Species: *Paidopithex rhenanus*, Pohlig 1895

The femur of *Paidopithex rhenanus* was provided by the Hessische Landesmuseum Darmstadt. It was discovered in 1820 in a sand pit of upper Miocene age, near the small village of Eppelsheim in Rheinish Hesse. Therefore, it is also known as Eppelsheimer femur. It was the first fossil hominoid ever found. Ernst Schleiermacher, founder and curator of the natural historic collection of the grand duke in Darmstadt, in which the specimen is housed since this time, interpreted it as a femur of 12 year old girl. He sent a cast and drawings of the specimen to George Cuvier in Paris for analyses. Unfortunately Cuvier never answered (Franzen 2000).

Later on, an intensive discussion began regarding the classification of the specimen. Citing Gieseler (1926), Schleiermacher and Kaup estimated that the specimen belonged to the fossil genus *Dryopithecus*. However, Richard Owen compared the femur with the hylobatids (Pohlig 1895, Gieseler 1926). Pohlig initially agreed in 1892 with the opinion of Schleiermacher and Kaup, but rejected Owen's interpretation (after Gieseler 1926) and assumed for the first time that due to its morphology the Eppelsheimer femur belonged to a primate which was more similar to modern humans than to living anthropoids. Thereupon he interpreted a habitual practice of biped locomotion for this species. Then in 1895, Pohlig rejected the estimation of Schleiermacher and Kaup, due to new findings of *Dryopithecus* and the since determined differing geological ages of the *Dryopithecus* and *Paidopithex rhenanus* sites. He confirmed and extended his opinion that the femur belonged to an anthropoid which resembled modern humans more than gorilla, chimpanzee or *Dryopithecus* do. He proposed the name *Paidopithex rhenanus* for the Eppelsheimer femur with respect to the first assumption of Schleiermacher that it belonged to a child (Pohlig 1895). Dubois (1895) disagreed with Pohlig's opinion about the locomotor interpretation and the morphological resemblance. Instead he emphasized, like Owen, the similarities with hylobatid femora and also noticed the larger size of the Eppelsheimer femur compared with the hylobatids. He proposed the name *Pliohylobates eppelsheimensis* for this specimen, but due to page priority the designation *Paidopithex rhenanus* is now commonly used.

The first x-ray investigations of the *Paidopithex rhenanus* femur by Walkhoff (1904), found additional evidence for the speculation of Owen and Dubois in the spatial arrangement of the cancellous bone. Walkhoff rejected Pohlig's interpretation and noted further that the radiography of the femur revealed that it was elongated by approximately 15 mm by the cement used to fix the fragments. After morphological and morphometrical comparisons of the

external shape of the Eppelsheimer femur with different catarrhini, GIESELER (1926) indicated that the fossil femur was comparable with hylobatids. On the basis of additional x-ray comparisons of anthropoid femora and the Eppelsheimer femur, he stated further that this fossil species did not practice an upright walking. In 1951 LE GROS CLARK & LEAKY compared the proportions and morphology of the *Paidopithex rhenanus* femur with fossil fragmentary femora of Maboko Island which were assumed to belong to *Proconsul*. SIMONS & PILBEAM (1965) and SZALAY & DELSON (1979) grouped the Eppelsheimer femur again with *Dryopithecus*. After a morphometrical analysis of the specimen by MCHENRY & CORRUCCINI (1976), similarities with *Pliopithecus* and *Hylobates* were found and as such they classified it as hylobatine. AIELLO (1981) compared femoral morphology of *Paidopithex rhenanus* and *Proconsul sp.* with below-branch feeders, including hylobatids and the New World genera *Alouatta*, *Ateles*, *Lagothrix*. She further interpreted both fossil species as ideally preadapted "..to the development of bipedal locomotion." (page 89), due to their relatively long femora as in comparison to extant great apes.

In 1992 BEGUN concluded from morphological analyses that the Eppelsheimer femur is rather similar to atelines and *Pliopithecus* than to hylobatids. Therefore, he estimated that *Paidopithex rhenanus* belonged to the Pliopithecidae and, that the specimen possessed no specific hominoidean features. In a functional interpretation he proposed that the extinct animal could have practised agile and speedy movements and also concluded that the hind limbs might have been habitually in suspended postures. Due to its similarities with *Pliopithecus*, he interpreted that *Paidopithex rhenanus* exhibited a positional behavior comparable with *Alouatta*. ANDREWS et al. (1996) rejected Begun's opinion and assigned the Eppelsheimer femur again to the Dryopithecinae.

A locomotor classification is hard to give for a single bone. The classical method of locomotor interpretation of fossils needs almost complete fossil skeletons. The features of extant species skeletons are thereby used to infer on the locomotor preferences of fossils. Concerning the Eppelsheimer femur, the problematic in this connection is striking, as just this single femur was ever found of the species *Paidopithex rhenanus*.

Description of the site of Eppelsheim

The site of Eppelsheim is located in the southeastern part of the Mainz Basin in western Germany. During the late Miocene, fluviatile sediments known as "Dinotheriensande" were deposited here. The geographical extension of the "Dinotheriensande" marks the course of a Miocene river system which runs at Eppelsheim roughly in a SE - NW direction (FRANZEN 2000). The "Dinotheriensande" are the earliest sediments of the Miocene Rhine river south of the Rhenian Slate Mountains ("Rheinisches Schiefergebirge"). They consist of sands and conglomerates with intercalated lenses of claystone. Sand pits have delivered thousands of mammalian fossils from the 18th to the early 20th century (FRANZEN 2000). Eppelsheim belongs to

the earliest known fossil mammal localities of the world. It was here that the first fossil hominoid, the Eppelsheim femur of *Paidopithex rhenanus*, was discovered. The "Dinotheriensande" are allocated to the European Land Mammal Mega Zone of the Vallesian (early late Miocene), and were, until recently, assigned to the lower part of the Neogene Mammal unit MN 9 (Mein 1986, Steininger 1999). Franzen et al. (2003a) concluded on the basis of recently discovered micromammals that the "Dinotheriensande" are deposited near the end of MN 9, implying that they are only about 9.5 instead of 10.5 Ma old.

The first scientific excavations in Eppelsheim were initiated by J. L. Franzen and G. Storch in 1996 (Forschungsinstitut Senckenberg). Numerous drillings helped to identify the distribution of the "Dinotheriensande" in this area (Franzen 2000, Franzen 2002, Franzen et al. 2003b). Those drillings have shown that the Miocene river was approximately 45-60 m wide. However, it was not possible to relocate the exact site where the Eppelsheim femur was discovered. In any case, the present excavation site lies close by, as the contours of old sand pits were discovered during recent excavations. The excavations have been run co-operatively by the Landessammlung für Naturkunde Rheinland-Pfalz and the Forschungsinstitut Senckenberg since 2001.

At the present site (Figure 2.11) the "Dinotheriensande" occur below 2-3 meters of loess. The site is bordered to the SW by the Miocene river bank which is built of the limestone deposits known as "Inflataschichten" (approx. 20 Ma) (now "Rüssingen Formation") of the early Miocene. Normally, these strata together with the early Miocene and late Oligocene limy deposits of the "Cerithienschichten" should follow in stratigraphic order underneath the "Dinotheriensande" (Franzen 2002). Instead, claystone, bearing marine Foraminifera as well as freshwater ostracodes typical of the late Oligocene "Süßwasserschichten" (26-28 Ma of age) are found underneath the "Dinotheriensande". Evidently a large hiatus of about 17 Ma exists between the "Süßwasserschichten" and the "Dinotheriensande". Following the interpretation of Franzen (2002) this hiatus results mainly from extensive carstification triggered by the "Süßwasserschichten" as a damming horizon. As such, the limy deposits of "Inflataschichten" and the "Cerithienschichten" were eroded and the Rhine river may have started as a cave river in that area .

Figure 2.11: Present excavation site of Eppelsheim, photograph by Elke Pantak-Wein

Chapter 3

Methods

The outer bone morphologies of the samples were described by conventional quantitative and qualitative methods as explained in chapter 3.1 and 3.2. The techniques described in chapter 3.3, 3.4, and 3.5 were used to investigate of the trabecular architecture.

3.1 Morphological description of bone shape

The exterior shape of the investigated femora was described morphologically. This description focused on morphological details which could not be depicted completely in the photographs made of each specimen. It follows the description of the human femur by Platzer et al. (1986) (Figure 3.1). The shape and course of the following features are therein included:

- shape of the shaft of the femur
- *Facies anterior*
- *Facies medialis*
- *Facies lateralis*
- *Labium laterale*
- *Labium mediale*
- *Linea aspera*
- *Caput femoris*
- *Fovea capitis*
- *Collum femoris*
- *Trochanter major*
- *Fossa trochanterica*
- *Tuberculum quadratum*
- *Linea intertrochanterica*
- *Crista intertrochanterica*
- *Trochanter minor*
- *Tuberositas glutaea* (*Trochanter tertius*)
- *Linea pectinea*
- *Facies patellaris*
- *Linea intercondylaris*
- *Epicondylus lateralis*
- *Epicondylus medialis*
- *Condylus lateralis*
- *Condylus medialis*
- *Fossa intercondylaris*
- *Facies poplitea*
- *Tuberculum adductorium*
- *Sulcus popliteus*

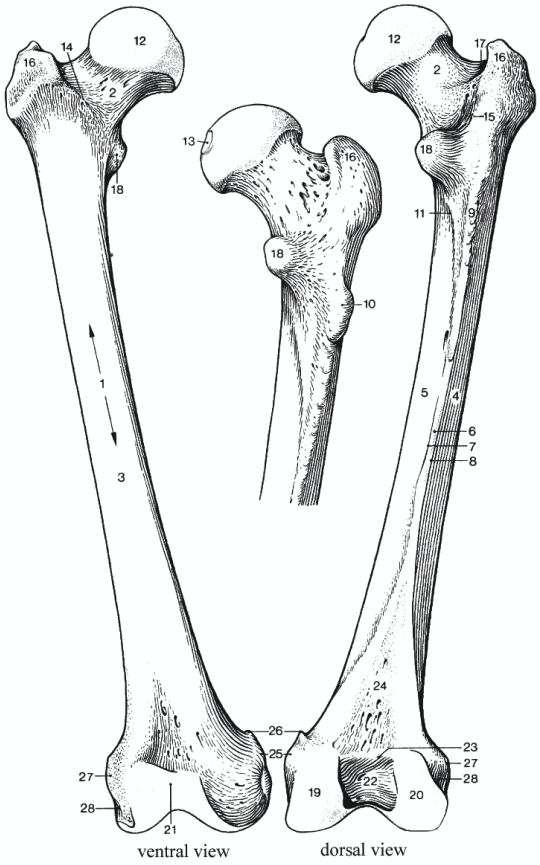

Figure 3.1: Characteristic features of the human femur after Platzer et al. (1986)

1. *Corpus femoris*
2. *Collum femoris*
3. *Facies anterior*
4. *Facies lateralis*
5. *Facies medialis*
6. *Linea aspera*
7. *Labium mediale*
8. *Labium laterale*
9. *Tuberositas glutaea* (*Trochanter tertius*)
10. *Tuberculum quadratum*
11. *Linea pectinea*
12. *Caput femoris*
13. *Fovea capitis*
14. *Linea intertrochanterica*
15. *Crista intertrochanterica*
16. *Trochanter major*
17. *Fossa trochanterica*
18. *Trochanter minor*
19. *Condylus medialis*
20. *Condylus lateralis*
21. *Facies patellaris*
22. *Fossa intercondylaris*
23. *Linea intercondylaris*
24. *Facies poplitea*
25. *Epicondylus medialis*
26. *Tuberculum adductorium*
27. *Epicondylus lateralis*
28. *Sulcus popliteus*

3.2 Morphometrical description of bone surface

The following parameters were measured on the samples for quantitative morphometric description. Each parameter was taken five fold to reduce variations in measurements. This selection of common morphometric parameters consists of parameters described by Duerst (1926), von den Driesch (1982), and Ruff (1988) (Figure 3.2). The distances A-D and F are based on von den Driesch (1982), with small variations in A and D. Parameters E, G and H are taken from Duerst (1926), with some modification in G.

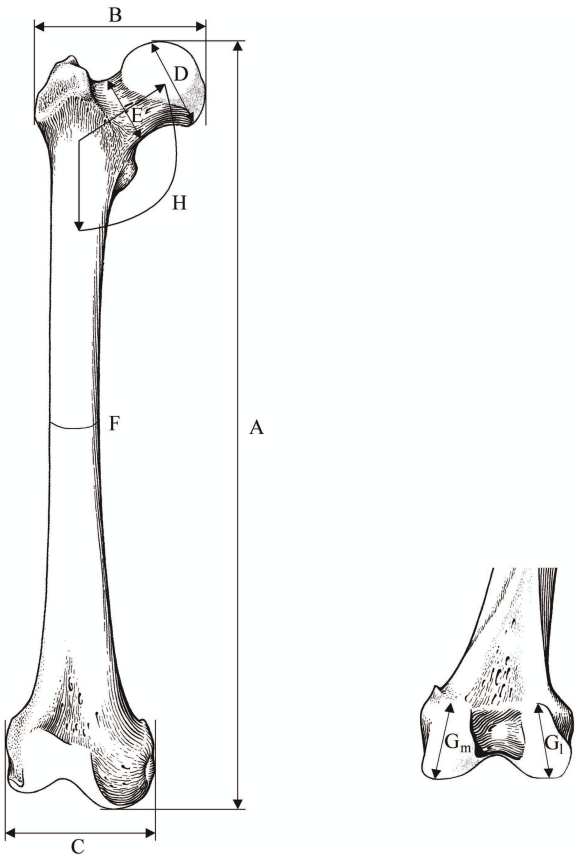

Figure 3.2: Measured parameters A-H depicted on a right human femur; sketch of the femur after Platzer et al. (1986)

A : Maximal longitudinal length [mm]

B : Maximal proximal width [mm]

C : Maximal distal width [mm]

D : Maximal height of the *Caput femoris* [mm]

E : Minimal diameter of the *Collum femoris* [mm]

F : Minimal perimeter of the diaphysis [mm]

G_l : Longest chord of the *Condylus lateralis* [mm]

G_m : Longest chord of the *Condylus medialis* [mm]

H : Angle between *Corpus femoris* and *Collum femoris* [°]

The measurements A-E were taken with calipers with the sample laying on its dorsum. A and D were measured with the calipers held in a parallel position to the shaft axis, while for B and C the calipers were held at a right angle to the shaft axis. For F and G, a measuring tape was used. The parameter H was acquired on different medio-lateral sections of the 3D CT images with the software VGStudio MAX (Volumegraphics, Germany) using a goniometric tool.

3.3 High resolution computed tomography

Whitehouse et al. (1971) and Whitehouse & Dyson (1974) noted the limited significance of studies depicting the spatial trabecular architecture in two-dimensions, such as provided by thin sectioning. They tried to minimize this limitation by the use of scanning electron microscopy. Further efforts to image and investigate the trabecular architecture in three dimensions gave rise to the surface stained block grinding technique (Vogel et al. 1989). Due to its dependence on cut surfaces, this method gives no insight into the spatial organization of whole bone trabeculae. Another disadvantage is the destruction of the sample during processing.

A recently developed alternative to time consuming, labor-intensive, and destructive sectioning techniques is high resolution computed tomography (CT). High resolution CT imaging provides detailed three-dimensional imaging of the spatial structure in cancellous bone, which is indispensable for more detailed analysis of the trabecular architecture (Compston 1994). As this method is non-destructive, the material can be used for future investigations, which is particularly important for fossil specimens. High resolution CT enables further the direct qualitative and quantitative analysis of a complex spatial structure like cancellous bone, which cannot be accomplished by section images and 2D histomorphometry (Borah et al. 2001). High resolution CT has already been applied for this purpose in medical sciences (Goulet et al. 1994, Guldberg et al. 1997a, Müller et al. 1998, Stenström et al. 2000, Borah et al. 2001, van der Linden et al. 2001) and recently in anthropological studies (Fajardo & Müller 2001, Ryan & Ketcham 2002a, Ryan & Ketcham 2002b, MacLatchy & Müller 2002).

The above studies were carried out with medical biopsy microcomputertomography systems, which are optimized for extant bone material. However, fossilized material requires special CT imaging conditions which are not matched by these systems (Scherf 2000, Scherf et al. 2005). During the fossilization process, bone material is altered by exchange processes. These processes can be part of more or less complete recrystallization. The inorganic component of extant bone consists of calcium hydroxy apatite ($Ca_{10}(PO_4)_6(OH)_2$). During fossilization a substitution between hydroxide (OH^-) and fluoride (F^-) or even chloride (Cl^-) tends to occur.

The phosphate group (PO_4^{3-}) is often replaced by carbonate (CO_3^{2-}). Under special conditions the calcium in the apatite is exchanged with other metal ions. The apatite might also be replaced more or less completely by another mineral phase, like pyrite (FeS_2) for example. Contact with acidic groundwater containing significant amounts of iron can cause vivianite ($Fe_3(PO_4)_2 \cdot 8H_2O$) facings. The medullary cavity, inclusive of the space between the trabeculae, is often filled as well. Depending upon the surrounding sediment and ion content of the pore water, these fillings can be composed of different minerals like pyrite, calcite ($CaCO_3$), sphalerite (ZnS), or barite ($BaSO_4$) (Martill 1991). Both conditions, the alterations of the former bone substance and the fillings, cause a higher X-ray absorption rate of the specimen and hinder CT imaging techniques.

In order to adapt to the unique conditions of fossilization, the fossil samples had to be imaged with a special CT system. For consistent results the extant samples were imaged with the same machine. The high resolution computed tomography system RayScan 200 of Hans Wällischmiller GmbH (Germany) at the FH Aalen, Arbeitsgemeinschaft Metallguss matched the requirements (Figure 3.3). This system was designed for material control of a wide range of objects. The microfocus X-ray tube of the RayScan 200 is infinitely variable up to 250 kV and provides a cone-beam X-ray (Simon et al. 2001). The higher output of the X-ray source, compared to medical biopsy systems yields better results for fossil specimens. The RayScan 200 permits imaging of samples up to a maximum size of 600 mm (Simon et al. 2001). This offers the chance to image whole bones of medium to large size species which can not be imaged by biopsy systems.

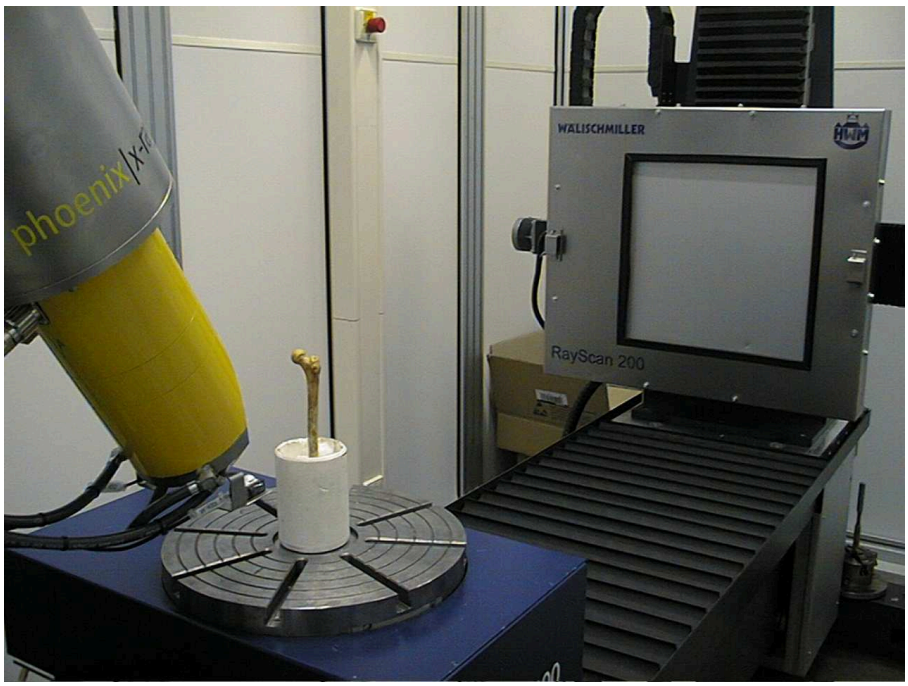

Figure 3.3: RayScan 200 at the FH Aalen, (Germany), with a mounted specimen

The RayScan 200 is equipped with an amorphous silicon area detector with 1024 x 1024 elements. In contrast to linear detectors, a nominal resolution of 5 μm can be achieved (personal communication M. SIMON, Hans Wällischmiller GmbH), which is of extreme importance for the calculation of histomorphometric parameters. PEYRIN et al. (1998) showed that a spatial resolution of 14 μm is needed to compute histomorphometric parameters reasonably. As the spatial resolution is influenced by the size of a specimen, this demand can only be accomplished in small biopsy samples that are gained only by the destruction of the whole specimen. This operation contradicts the purpose of this study, and is not suitable for fossil material. Biopsies also give only a limited insight into the complex cancellous bone network and are in this way unsuitable for the present study. The trabecular architecture must be seen as a whole system as its spatial structure transmits loads from different directions. Concerning the investigation of whole bones from lager specimens a resolution worse than 14 μm is inevitable, as the resolution scales with the size of the specimen. As long as no microcomputertomographic system can provide a resolution of 14 μm, the system with the best obtainable resolution will provide the most accurate data.

Before imaging the samples were mounted on a turntable with special attention paid to vertical alignment of the shaft axis along the z-axis of the imaged volume. A preliminary test has shown that oblique alignment of a specimen enhances the image resolution due to better exploitation of the detector area. However, to compare images of different specimens reasonably, an uniform alignment of the objects is essential as a virtual reorientation of the test image caused a decrease in resolution. A consistent vertical position of the samples shaft axis during the imaging procedure seemed advisable.

To ensure optimal and artifact free images, regular system adjustments were conducted before imaging. Of each sample, the proximal part of the femur, from head to end of lesser trochanter was imaged. To obtain optimal image quality, despite limited computer memory capacity, the raw data of each image was separated into two equal and successive parts which were reconstructed separately afterwards. Special attention was taken to ensure the parts had the same image properties and aligned equally, which was necessary to allow the final 3D reconstruction. Preceding tests outlined the numerous problems which occur if these arrangements are not considered. One problem, for example, were inconsistent centers of rotation of successive image parts, which disabled the merging operations and made consistent preprocessing of the 3D image inapplicable. A survey of the samples specific resolutions gained through this method are given in table 3.1.

The resolutions of the CT images differ between the samples in accordance to the sample size. KOTHARI et al. (1998) and PEYRIN et al. (1998) have shown that the resolution of CT images influences the accuracy of histomorphometric analysis. The comparison of histomorphometric data gained from images with equal resolutions therefore seems reasonable. However, when investigating species of different sizes, it must be taken into consideration that trabecular dimensions may scale with body size as a consequence of the mechanical adaptation of can-

Table 3.1: Resolutions of the high resolution CT images

Sample	Resolution [mm]
Alouatta seniculus 25 545 l	0.037
Alouatta seniculus 25 544 l	0.032
Alouatta seniculus 69.19 l	0.037
Presbytis entellus 4734 l	0.048
Presbytis entellus 4745 l	0.037
Presbytis entellus 4746 l	0.037
Papio hamadryas 1.553 l	0.045
Papio hamadryas Ha VIII.83 l	0.061
Papio hamadryas Ha VIII 3 l	0.060
Papio hamadryas 3212 l	0.061
Hylobates syndactylus 6983 l	0.043
Hylobates syndactylus 52.36. l	0.044
Hylobates lar moloch 47 979 r	0.038
Homo sapiens 10 l	0.106
Homo sapiens 11 l	0.121
Homo sapiens 21 l	0.121
Homo sapiens 22 l	0.106
Pliopithecus vindobonensis O.E. 304 r	0.042
Pliopithecus vindobonensis O.E. 559 l	0.044
Pliopithecus vindobonensis O.E. 560 l	0.044
Pliopithecus vindobonensis 1970/1397/22 r	0.044
Pliopithecus vindobonensis 1970/1397/23 l	0.044
Pliopithecus vindobonensis 1970/1398/2 l	0.044
Paidopithex rhenanus Din 45 r	0.056

cellous bone. In accordance with a decrease in body size, the loads applied to the bone are expected to decrease also. Unfortunately no study investigating this issue in particular has been carried out up to now. Therefore, it is considered indispensable to image the specimens with the highest obtainable resolution in order to image the cancellous structure accurately. The intentional limitation of resolution in smaller specimens which would enable the matching of resolution in bigger specimens, would yield inadequate results. Due to the partial volume effect, some structures would appear bigger than actual and very fine structures would be deleted in the CT image.

3.3.1 Definition of the Region of Interest (ROI)

Merging, defining regions of interest (ROI) and presentation of the images obtained with the RayScan 200 system was accomplished with the software system VGStudio MAX (Volumegraphics, Germany). After the merging, an anatomically comparable ROI, located in the region of the lesser trochanter, was defined for each specimen. Former investigations of Fajardo & Müller (2001), Ryan & Ketcham (2002a), Ryan & Ketcham (2002b), and MacLatchy & Müller (2002) focused on the femoral head and neck. In this way the effects of loads induced by body weight and the combined muscle forces which push the femoral head into the acetabulum were taken into account. Therefore two interfering loading conditions, caused my muscles and by body weight, has to be considered in the femoral head and neck. Simple loading conditions should be more appropriate to investigate the influence of locomotor loading on cancellous bone. Additionally, femoral head and neck are not directly subjected to the muscle loads which act on the trochanters and directly on the corpus femoris. These loads are clearly significant during locomotion, as the muscles are involved in locomotor processes. As the muscles for extension, inward and outward rotation, and abduction insert at the greater trochanter, this region seems at first sight an optimal region of interest. However, the shape and size of the greater trochanter varies considerably in the sample group, hindering the definition of an anatomically and functionally similar ROI. For example *Alouatta seniculus* (Figure 4.1) has a very slender and small greater trochanter in relation to *Presbytis entellus* (Figure 4.7). Alternatively, the region around the lesser trochanter is rather easy do define as it is similar in all specimens. By the insertion of the flexor muscles into the lesser trochanter locomotion related features are expected in this region, too. Therefore, the region around the lesser trochanter was chosen as ROI in this study.

The ROI differ slightly between the specimens due to the different dimensions of the specimens and variations in their outer bone morphologies. The vertical heights of the ROI were defined by the following procedure. First, the maximal projected width of the trochanter minor in each specimen was measured in a sectional view along the z-axis (axial view). The distance was measured parallel to the dorsal side of the femur (Figure 3.4). A ratio of $1.5 \pm 5\%$ between the maximal projected width and the vertical heights of the ROI was found to be suitable to define the shafts parallel extension of the lesser trochanter and the ROI, respectively. The derived formula is therefore: $\frac{w}{(1.5 \pm 5\%)} = h$ (w: maximal projected width, h: vertical heights). A

tolerance of ± 5% was necessary to enable the adjustment of the ROI to individual variations. At the end of the procedure a visual comparison of the specimens was made to check that the ROIs were similar.

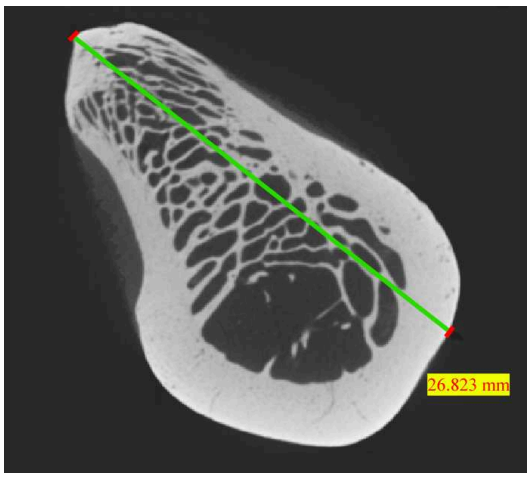

Figure 3.4: Measured distance of the maximal projected width of the trochanter minor area of *Papio hamadryas* (Ha VIII 83 l)

3.3.2 High resolution computed tomography with synchrotron radiation - SR-μCT

As already mentioned in chapter 1.2, mineral distribution is a critical factor influencing the material properties of bone. To check the mineral distribution in trabecular bone and to estimate their variation, a preliminary study was carried out on samples of the right femora from four individuals of this study (25 544 r ♀, 25 545 r ♀, 10 r ♀, 11 r ♂). A special high resolution CT facility, operating with synchrotron radiation, was used at the HASYLAB at DESY (Hamburg) in cooperation with Dr. Beckmann (GKSS), and Dr. Witte and Dr. Fischer from the department of orthopaedic surgery (Hannover Medical School) (Scherf et al. 2004). This study confirmed the assumption that by using high resolution computed tomography with synchrotron radiation, it is possible to obtain more accurate information about the composition and therefore mineralization grade of the bone substance. This is because SR-μCT provides a higher spatial resolution and better differentiation of the bone mineral density. Another cooperative study with Dr. Witte and Dr. Fischer concerning the composition of bone on micron level is ongoing.

Studies about the applicability of SR-μCT to analyze the trabecular architecture have increased in the last years (Bonse et al. 1994, Salomé & Peyrin 1999, Peyrin et al. 2001). The benefits of such a system working with synchrotron radiation compared to systems with conventional x-ray sources depend on the high intensive, monochromatic, and parallel aligned synchrotron radiation (Dalstra et al. 1999). Despite these advantages, studies on large samples are not realizable, due to the extremely time consuming imaging procedure, the rarely accessible beamtime and the quite large 3D image data.

3.4 Histomorphometry of high resolution CT images

3.4.1 Preprocessing of the fossil specimens

Before the histomorphometrical analysis of the fossil specimens ROI could start, their filling had to be separated and deleted. These fillings were caused partly by fossilization and in some samples by the glue fixing the fragments. By virtue of their origin, the fillings are composed of different materials. Unfortunately, there exists no digital segmentation program designed for such inhomogeneous materials on par with fossil fillings. Their segmentation had to be accomplished by a grey value based segmentation tool and by manual segmentation operations with VGStudio MAX.

The complete removal of the ROI filling in a specimen would have taken several weeks. To reduce the amount of work involved in segmentation, a particular working routine was conceived. Only those parts of the filling which have a similar grey value, corresponding to a similar absorption coefficient as the fossil bone material were considered for individual segmentation. Filling materials with markedly lower grey values compared to the fossil bone were suppressed by an automatic grey value threshold. The grey value spectra of the former bone material unfortunately varied considerably in almost every fossil specimen. This made individual segmentation of the majority of the fillings necessary. The segmentation was carried out on section images of the z-axis (axial sections).

The different filling materials necessitated the application of different individual segmentation operations on the fossil specimens. For *Pliopithecus vindobonensis* 1970/1397/22 r, 1970/1397/23 l, and 1970/1398/2 l a consistent segmentation procedure could be applied. In a first step large filling areas were segmented by a three dimensional grey value tool with a region-growing algorithm. The tolerance was set to 300.00 with a variation of ±15% to adjust to local grey value variances in the filling. Afterwards, small filling areas which were not collected by the first step were segmented by a lasso tool. The transition areas between the filled and the unfilled space often exhibited grey values in the range of fossil bone. To segment these areas the grey value tool of the first step was used again with the same tolerance setting. Lasso segmentation was applied subsequently to collect remaining small areas and pixels which were not gathered in the former steps. Finally the lasso tool was used again to remove regions in fossil bone which were accidentally segmented during application of the grey value segmentation tool (Figure 3.5).

Compared to the former specimens, the filling of *Pliopithecus vindobonensis* O.E. 559 l was somewhat more discreet. The segmentation was accomplished by applying the grey value tool on the filling and its border areas in one step. The then undetected areas and pixels were acquired by the lasso tool. At the end, the lasso tool was used to delete misattributed pixels from the segmented volume. The ROI of *Pliopithecus vindobonensis* O.E. 304 r was segmented only by the lasso tool as just very small and isolated fillings occurred. The segmentation procedure for *Paidopithex rhenanus* Din 45 r was more sophisticated as the filling of this specimen was very heterogeneous. A nonlinear diffusion filter was first applied three times to decrease the differences

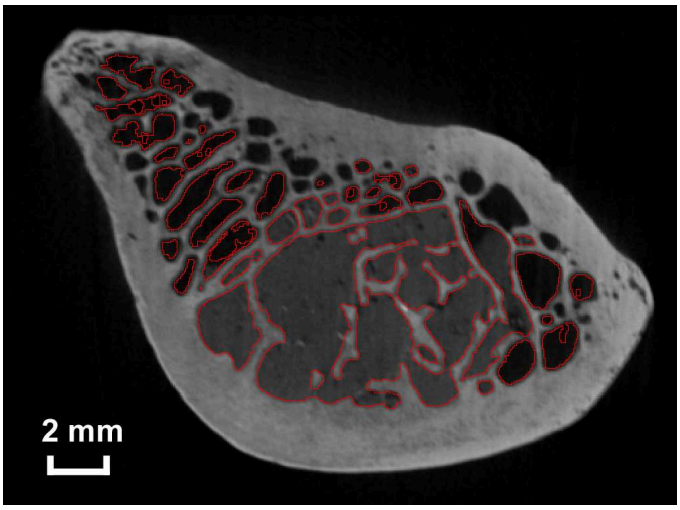

Figure 3.5: Example of a segmented slice of *Pliopithecus vindobonensis* 1970/1397/22 r

in the grey value spectra. The same procedure as for the samples 1970/1397/22 r, 1970/1397/23 l, and 1970/1398/2 l of *Pliopithecus vindobonensis* was then applied. The tolerance of the grey value tool had to be varied between 100.00 and 300.00 as the filling covered a larger grey value range compared to the former specimens even despite the filtering operations.

Only *Pliopithecus vindobonensis* O.E. 560 l, had to be excluded from the histomorphometric analysis. The image revealed a complete, massive filling which demonstrated the same absorptive properties as the fossil bone. A differentiation of bone and filling was possible by visual inspection of the CT sections but a complete segmentation of the ROI would have been too time consuming and beyond the scope of this project (Figure 3.6). Additionally, this specimen is damaged inferiorly and lacks some parts of the ROI.

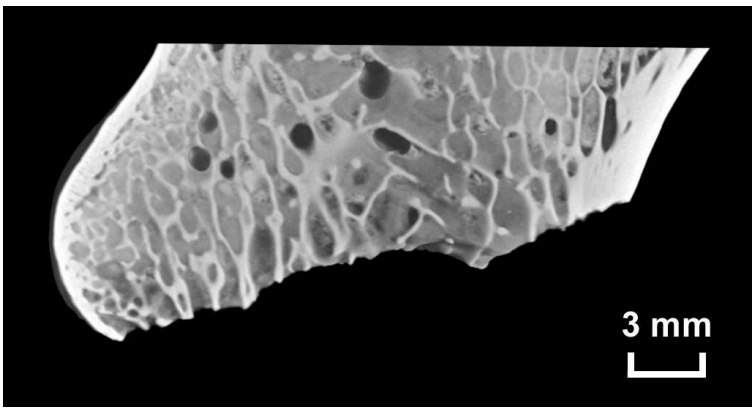

Figure 3.6: View on the trabecular architecture of the anterior half of the lesser trochanter and the filling of *Pliopithecus vindobonensis* O.E. 560 l

3.4.2 Histomorphometrical analysis of cancellous bone

The histomorphometrical analysis of the cancellous bone was accomplished by the SCANCO Medical AG (Switzerland) with software offering histomorphometric measurements directly on the specimen structure (Scanco 2005a). The software provided further segmentation of cancellous bone and cortical bone by a semi-automatic, standardized method described in Laib et al. (2000). This segmentation tool was applied to obtain consistently generated trabecular bone regions from the ROIs. However, the above mentioned variations in grey value spectra caused serious defects of those trabecular structures with very low grey values. These structures were in fact deleted by this operation. To decrease this problem and to include the deleted trabeculae in the analysis, the ROIs of the fossil specimens had to be subjected to an edge reinforcement filter incorporated in the SCANCO software. To enhance the result of *Paidopithex rhenanus* Din 45 r, an additional individual grey value adjustment had to be accomplished by SCANCO in advance. Afterwards the ROIs were histomorphometricaly analyzed. The analysis yielded the following parameters:

- 1) Tissue Volume (TV) [mm^3]
- 2) Bone Volume (BV) [mm^3]
- 3) Bone Volume Fraction (BV/TV) [%]
- 4) Connectivity Density (Conn.Dens) [$1/mm^3$]
- 5) Structure Model Index (SMI) [1]
- 6) Distances |H1|, |H2|, |H3| [mm]
- 7) Degree of Anisotropy (DA) [1]
- 8) Mean Trabecular Thickness (Tb.Th) [mm]
- 9) Mean Trabecular Separation (Tb.Sp) [mm]
- 10) Mean Trabecular Number (Tb.N) [1/mm]
- 11) Bone Surface (BS) [mm^2]
- 12) Standard Deviation of local Thicknesses [mm]
- 13) Standard Deviation of local Separations [mm]

The parameters 1)-3) and 8)-11) are common histomorphometric parameters (Parfitt et al. 1987), while the parameters 12) and 13) are additionally computed by the SCANCO histomorphometric analysis. The parameters 8)-10) are computed twofold by this analysis software. The first calculation is based upon a plate model and the second calculation refers directly to the 3D-image (personal communication A. Laib, SCANCO Medical AG). Parameters calculated on the basis of mathematical models, like for example the plate model, bear a source of error due to the assumed mathematical geometry of the structure (Goulet et al. 1994). Laib et

al. (2000) affirmed the discrepancy between directly calculated data and data computed by the assumption of a mathematical model. Therefore, only the values calculated directly from the 3D model were used for this study.

The method for direct calculation of 'trabecular thickness' (Tb.Th) (8) based on a 3D model was established by Hildebrand & Rüegsegger (1997a). The computation of 'connectivity density' (Conn.Dens) (4) refers to the method of Odgaard & Gundersen (1993) which was refined after Laib et al. (2000). The term 'connectivity' describes the number of connections between the trabeculae minus one connection. The 'connectivity density' is calculated as the relation of 'connectivity' to the analyzed volume. A quantitative description of the shape of the trabeculae, in terms of concavity or convexity, is given by the 'structure model index' (SMI) (5) of Hildebrand & Rüegsegger (1997b). As an expression of a convex structure, trabecular bone composed of ideal cylindrical trabeculae would generate a SMI of 3, whereas trabecular bone composed of ideal plate-like trabeculae would yield a SMI of 0. Concave structures, such as openings in plate-like structures cause negative values of the SMI (Scanco 2005b).

The distances |H1|, |H2|, |H3| (6) correspond with the 'mean intercept length' of Whitehouse (1974). |H1| is the minimal, |H2| the maximal, and |H3| the intermediate average distance between two interfaces (bone to non-bone) in the three different directions H1, H2, and H3 (Rüegsegger et al. 1996, personal communication A. Laib, SCANCO Medical AG). These directions are then computed by the SCANCO histomorphometric analysis. The relationship between the biggest and smallest distances usually yields the 'degree of anisotropy' (DA) (7). In this histomorphometric analysis, the 'degree of anisotropy' was instead calculated following the advanced method of Laib et al. (2000).

3.5 Finite Element Method (FEM)

FEM modelling should be used in this work to clarify the main femoral loading conditions since the specific load environment of a bone can not yet be determined in detail (Rubin et al. 1990, Rafferty 1998). Investigations are commonly regarding femoral loading conditions only for the human body. These are based on electromyographic studies analyzed with the aid of mathematical models (Crowninshield et al. 1978) or on calculations of muscle features measured from cadavers (Jensen & Davy 1975, Brand et al. 1986). Data from in vivo measured joint forces are only available through instrumented implants (Davy et al. 1988, Kotzar et al. 1991, Bergmann et al. 1993). All these methods may demonstrate error due to flawed assumptions in their mathematical models, altered post mortem muscle features or alteration in loading conditions caused by implantation.

As the trabecular architecture is a complex three dimensional structure in which the various parts are loaded differently, a 3D FE mesh depicting all its architectural features is indispensable to analyze the mechanical behavior accurately. The complexity of the three dimensional structure and the limitations of PC memory capacity often place restrictions on 3D meshing and

modelling. To avoid conflicts with the PC memory capacity, many 3D FEM studies investigate trabecular bone separate from cortical bone (Guldberg et al. 1997a, Niebur et al. 2000, van der Linden et al. 2001, Jaasma et al. 2002, Newitt et al. 2002). The influence of cortical bone on the mechanical behavior of cancellous bone is usually therefore ignored. However, the mechanical behavior of bone is crucially influenced by the trabecular architecture and the surrounding cortical bone (Stenström et al. 2000). Therefore, it is indispensable to model the cortical together with the cancellous bone to provide a physiologically accurate model for mechanical analysis.

FE models of cancellous bone are often generated with the aid of a surface-fitting method, which describes the trabecular surface mathematically. However, utilizing the voxels of a 3D CT image is a more effective mesh generating method than the surface-fitting FE mesh generation. By this method, the individual voxels of a 3D CT image are used as individual elements of the FE model (Hollister & Kikuchi 1994). This offers the opportunity to generate exact FE meshes of cortical and cancellous bone structures without mathematical assumptions. FE meshes generated using high resolution CT images depicting single trabeculae with at least three to four voxel diameters are as good as previously used surface-fitting approaches (Guldberg et al. 1998) and can be obtained rather easily compared to the surface-fitting method. Thus, the FE meshes were generated in this study from the 3D high resolution CT images. In simulations of loading processes on virtual trabecular bone models, the changes in stress level of each element were then computed.

The generation of FE models and modelling simulations were accomplished by Dr. Baaser (today Freudenberg Forschungsdienste KG, Weinheim, formerly TU Darmstadt - Institute of Mechanics) via a cooperative project concerning stress and strain analysis in bone material. For mesh generation, the single voxels of the high resolution CT raw data were converted by the software vox2br (see http://coulomb.mechanik.tu-darmstadt.de/user/baaser/Forschung/vox2br.html) into 8 noded brick elements with a highly optimized code for evaluating the material model. Afterwards the models were loaded with differing stresses from various directions. Concerning the stress directed alignment of the cancellous bone, the predominate loading directions should be evaluated. With this information, conclusions about the origin of these loads by muscles and body weight, should be drawn.

Fischer et al. (1995) investigated the loading conditions on femora with a similar FEM analysis. They used a simplified epiphyseal 2D FE model to determine the loads which gave rise to the density distribution in the model. The study showed that this simplified method could not predict the exact loads but instead computed loading cases which were quite similar to the original ones. Recently, Ryan & van Rietbergen (2004) presented a similar approach by generating 3D FE models with high resolution CT images such as presented in this study.

As already mentioned in chapter 1.2 material properties are crucial in FE modelling. Due to the problem that no data exists regarding the material properties of non-human primate bone, data from humans had to be used instead. The assumption of Erickson et al. (2002) that

the material properties of long bones stayed quite the same throughout evolution, regardless of systematic groups does not appear credible especially with regard to the findings cited in chapter 1.2. Furthermore, only very sparse data exist on the maximum locomotor loading of different primate species. To verify the assumptions for the described FE method, a pilot study was first conducted.